Cu(II)-metalated Silica-based Inorganic-Organic Hybrid: Synthesis, Characterization and Its Evaluation for Dye Degradation and Oxidation of Organic Substrates

A. Naz,[a] S. Arun,[b] R. Kumari,[a] S. S. Narvi,[a] and M. S. Alam[c,*]

[a]Department of Chemistry, Motilal Nehru National Institute of Technology Allahabad, Prayagraj, Uttar Pradesh, India-211004

[b]Department of Chemistry, Dr. Shakuntala Misra National Rehabilitation University, Lucknow, Uttar Pradesh, India-226017

[c]Department of Chemical Engineering, Motilal Nehru National Institute of Technology Allahabad, Prayagraj, Uttar Pradesh, India-211004

A novel and efficacious inorganic-organic hybrid material was synthesized by immobilizing Cu(II)-Schiff's base complex on silica-gel using 3-(2-aminoethylamino) propyltrimethoxysilane as linker and 1,3-diphenyl-1,3-propanedione for Schiff's base formation. The hybrid was characterized by FT-IR, DRUV-Vis, Solid State ^{13}C CPMAS NMR, Powder-XRD, SEM, ICP-AES, EDX and TGA and EPR techniques. Catalytic ability of the hybrid was evaluated for oxidative degradation of Reactive Black 5, and oxidation of few representative organic substrates, viz., tetralin, cyclohexane, cyclohexanol, and cyclopentanol, where the hybrid catalyst decomposes H_2O_2 to generate ·OH free radicals. Influence of various reaction parameters, i.e., H_2O_2 concentration, catalyst concentration, and temperature, on dye degradation process was studied and best reaction conditions for maximum degradation of RB5 were also determined. The catalyst gave a high dye degradation efficiency of 91 %, and a good product yield of 42.61 %, 41.09 %, 40.54 %, and 38.44 % for conversion of tetralin (with selectivity of 74.23 % and 25.77 % for tetralone and tetralol, respectively), cyclohexane (with selectivity of 75.05 % and 24.95 % for cyclohexanone and cyclohexanol, respectively), cyclohexanol (with 100 % selectivity for cyclohexanone), and cyclopentanol (with 100 % selectivity for cyclopentanone), respectively. Easy separation, reusability, and good catalytic activity leading to possible development of eco-friendly industrial manufacturing process are the motivating factors for using the synthesized novel material.

Keywords:
inorganic-organic hybrid, silica gel, catalysis, Reactive Black 5, hydrogen peroxide

Introduction

Rapidly increasing environmental pollution, formation of hazardous substances, and a number of health related challenges in everyday life compels us to move towards green chemistry, and to synthesize such materials and equipment that could enhance the general well-being of individuals and the society. Development of inorganic-organic hybrid materials is one such approach. The combination of organic and inorganic species results in a material having synergistic effect of both the components. These materials have proved to be effective in many areas, such as barrier coatings, sensors, solar cells, catalysts, and medical applications[1–5]. The use of such hybrids as heterogeneous catalysts has been of great interest for researchers in the last decade. The hybrids may be synthesized by simple strategies. One strategy of these methods could be immobilizing organic moieties onto silica surface, an inorganic species. Silica gel serves as a good inorganic support owing to; (i) presence of adequate number of silanol groups to which desired organic molecules can be grafted, which can further be modified, (ii) high thermal resistance, (iii) grafted groups are covalently linked and therefore, resistant towards their detachment from the surface of silica through organic solvents or water, and (iv) organically modified SiO_2 gel usually facilitates and boosts the adsorption/coordinate bond formation of metal ions[6], thereby increasing their life span on silica surface[7]. Considering these, inorganic-organic hybrids may

*Corresponding author: Tel.: +91-532 2271584,
E-mail address: msalam@mnnit.ac.in

have good catalytic activity, which can be utilized in environmental remediation, such as waste/effluent treatment, along with enhancement in production capacity of various industrial processes.

In the present work, we have synthesized and characterized a novel silica based Cu(II) inorganic-organic hybrid compound, obtained by grafting Schiff's base onto silica surface and complexation of the base by Cu(II) chloride. The metal complex hybrid thus formed was successfully used as a heterogeneous catalyst for oxidative degradation of a non-biodegradable disazo dye, Reactive Black 5 (RB5), as well as in the oxidation of cycloalkanes (i.e., tetralin and cyclohexane) and cycloalcohols (i.e., cyclohexanol and cyclopentanol) by using in both cases hydrogen peroxide as an environmentally amiable green oxidant. To the best of our understanding, this may be regarded as a step towards a reusable inorganic-organic hybrid catalyst for solving the issues of environment as well as of chemical industries simultaneously.

These inorganic-organic hybrids may have found a valuable application as catalysts in the dye degradation[8,9]. Dyes being used in large amounts have adverse effect on biota due to their carcinogenic and toxic behavior, and thus their degradation is a challenge for healthy life. More than 50 % of all produced dyes are azo dyes[10] and among the azo dyes most widely used are azo reactive dyes having one or several azo (–N=N–) groups with substituted aromatic structures[11]. These reactive dyes are widely used in paper, ceramic, textile, pharmaceutical, and food processing industries. The effluents from these industries contain residual dyes, which need proper treatment before being finally released into the environment. Thus, synthesis of novel hybrid recyclable catalyst for treatment of such dyes has become a challenge in recent years. Various methodologies, such as adsorption[12], filtration process[13,14], electrochemical method[15], coagulation[16], advanced oxidation processes (AOPs)[17,18], etc., are being employed for the removal and degradation of dyes. However, the hazardous pollutants from dye wastewater can only be transferred from one phase to another by these techniques, and it is difficult to degrade them through biological treatment processes[19]. Thus, the final environmental problems remain unresolved by these techniques and, therefore, processes leading to complete mineralization of dyes or their degradation to less harmful compounds are recommended to solve the problem. AOPs using homogeneous catalysts have emerged as a useful method for destruction of such toxic pollutants, where using highly reactive ·OH radicals for driving oxidation process is the characteristic feature of all AOPs[20]. However, certain problems are associated with homogeneous catalysts, such as difficulty in

their separation from reaction mixture. This has forced research groups to move towards insoluble catalysts. Novel hybrid recyclable heterogeneous catalysts can lead to a better approach towards environmental remediation in treating toxic dyes, and therefore, their synthesis has become a challenge in recent years.

The heterogeneous catalysts have also proved to be more viable for oxidation of various alkyl aromatic compounds, cycloalkanes, cycloalkenes, cycloalcohols, sulphides, olefins, etc.,[21,22] in certain industrial processes. Selective conversion of cyclohexane to cyclohexanone and cyclohexanol is an important requirement in chemical industry for the synthesis of Nylon-6,6 and Nylon-6 polymers, where ε-Caprolactam, an essential precursor of Nylon-6 and plastics, can be directly synthesized from cyclohexanol[23]. Cyclopentanone, oxidative product of cyclopentane, is used to synthesize pyridine, pyran, and thiophene derivatives, which exhibit cytotoxicity against some cancer cell lines[24]. Tetralone, a keto derivative of 1,2,3,4-tetrahydro-naphthalene (tetralin), is an important reactive intermediate for materials such as dyes, agrochemicals, and pharmaceuticals[25]. Immobilization of metal complex catalyst over inorganic support is a new strategy, and has the advantage of being selective and efficient as the common advantages of most metal complex catalysts. In continuation of our earlier paper[26], where we had reported the Cu(II) containing Schiff's base functionalized inorganic-organic hybrid and its potential application as anti-bacterial agent and as catalyst for dye degradation, we are reporting a new hybrid as catalyst for dye degradation and organic transformation.

Materials and methods

Materials and characterization techniques

Silica gel (Sigma Aldrich, India, Davisil Grade 923) with particle size of 100–200 mesh and pore diameter of 30 Å (surface area = 430–530 m^2 g^{-1}) was used. 1,3-diphenyl-1,3-propanedione (DPPD, 98 % purity), anhydrous CuCl$_2$ (≥99.995 % trace metals basis; anhydrous grade) and Reactive Black 5 (RB5, Dye content ≥ 50 %) dye, 3-(2-aminoethyl-amino) propyltrimethoxysilane (AAPTS, Technical grade, ≥80 %) were purchased from Sigma Aldrich, India. Hydrogen peroxide (30 % w/v, analytical reagent), toluene (99.5 %, analytical reagent), glacial acetic acid, dimethyl sulfoxide, dimethylformamide, and acetonitrile were procured from CDH (Central Drug House (P) Ltd., India). The concentration of hydrogen peroxide (w/v 30 %) was verified through iodometric titration; H$_2$O$_2$ solution was then used for the reaction. Substrates used for oxidation reac-

tion, i.e., tetralin (98.0 %, Laboratory Reagent), cyclohexane (99.5 %, Analytical Reagent), cyclohexanol (99.0 % Analytical Reagent), cyclopentanol (99.0 %, Synthesis grade) were also purchased from CDH, India. Ethanol ($\geq$ 99.9 %) was bought from Merck. All the chemicals were used without purification, except toluene, which was firstly made pure and then used.

Perkin Elmer spectrophotometer (Spectrum Two) was used to obtain FT-IR spectra in the range of 4000–400 cm^{-1}, using KBr disks. ^{13}C NMR spectral studies were performed at 100.52 MHz by ECX-Jeol 400(S), AVIII400(L) NMR spectrometer. SEM and EDX analyses were performed by CARL ZEISS EVO 50 coupled with Silicon Drift EDS detector fitted with a backscattered electron detector. The samples were coated with thin gold layer before performing SEM analysis. Diffuse reflectance UV-visible spectra were obtained by Shimadzu UV-3600 Plus UV-VIS-NIR spectrophotometer, using BaSO$_4$ as reference. Dye concentration was also measured on the same UV-Vis instrument, with optical path length of 1 cm. Milli-Q water was taken as reference for these analyses. The content of copper in the hybrid was analyzed through SPECTRO Analytical Instruments GmbH-ARCOS, Simultaneous ICP Spectrometer. Room temperature EPR analysis was performed through ES-DVT4 Spectrometer at 9.167 GHz, using DPPH as standard (g = 2.0036). Thermogravimetric analysis was performed under a dynamic N$_2$ atmosphere in the range of 30 °C–800 °C at a heating rate of 10 °C min^{-1} on a Perkin Elmer STA6000 system. Powder-XRD patterns were recorded on Rigaku SmartLab X-ray diffractometer at 25 °C, using step time of 1.0000 second, step size [°2θ] of 0.0200º and 2θ with a scan angle from 5º to 80º. The products obtained after substrates oxidation were analyzed by GC-Mass spectrometry (GC-MS) using Thermo Scientific TSQ 8000 gas chromatograph-mass spectrometer.

Hybrid synthesis

The hybrid was synthesized as follows:

Silica gel activation (SiO$_2$)

Silica gel was activated according to the literature[27]. Typically, an excess amount (50 mL) of 1:1 (conc. HCl):H$_2$O (v:v) was added to silica gel (6 g) and refluxed for 6 h at 105 ºC ($\pm$ 1 ºC). The suspension was filtered and the solid was washed with Milli-Q water until pH 7 was attained, the pH was monitored by pH meter. Silica gel was finally dried at 120 °C ($\pm$1 °C) for 12 h in hot air oven. The activation of silica gel was verified by FTIR analysis which showed surface silanol stretching vibrations at 3442 cm^{-1} and surface silanol bending vibrations[27] at 1639 cm^{-1} (Fig. 1a).

*Synthesis of amino-functionalized silica gel (SiO$_2$*NH$_2$)*

The immobilization of 3-(2-aminoethylamino) propyltrimethoxysilane (AAPTS) on silica gel was achieved by slightly altering the method as reported by Antony *et al.*[7] The activated silica gel (5 g) and solution of AAPTS (23.12 mmol) in anhydrous toluene (25 mL) were mixed and the suspension was refluxed for 24 h at 115 $\pm$ 1 ºX under N$_2$ atmosphere and filtered. The solid was washed with toluene, ethanol, and diethyl ether. Soxhlet extraction was performed with a 1:1 solution of ethanol and dichloromethane (DCM) to remove any silylating reagent residue adsorbed on silica surface. It was then dried at 50 °C ($\pm$1 °C) under vacuum. FTIR was recorded to confirm the grafting of organic moiety, which showed C–H stretching vibrations at 2901 cm^{-1}, C–H bending vibrations at 1490 cm^{-1} and NH$_2$ bending vibrations[27,28] at 1551 cm^{-1} (Fig. 1b)

*Modification of amino-functionalized silica gel with DPPD (SiO$_2$*NH$_2$*DPPD)*

A solution of 1,3-diphenyl-1,3-propanedione (DPPD, 0.893 mmol) in anhydrous ethanol (30 mL) was added to 1 g of the synthesized SiO$_2$*NH$_2$ compound. The suspension was refluxed for 24 h at 85 $\pm$ 1 ºC and filtered. The pale yellow powder was repeatedly washed with ethanol, and then Soxhlet extracted with ethanol and DCM, respectively, for 12 h to remove any unreacted DPPD. It was then vacuum dried at 70 °C ($\pm$1 °C).

*Metalation of Schiff's base functionalized silica hybrid by Cu(II) (SiO$_2$*NH$_2$*DPPD*Cu)*

The copper(II)-incorporated hybrid was prepared by refluxing a mixture of anhydrous CuCl$_2$ (0.508 mmol) and SiO$_2$*NH$_2$*DPPD (1 g) in anhydrous ethanol (20 mL) at 85 $\pm$ 1 ºC for 24 h. The obtained dark green colored solid material was filtered and then Soxhlet extraction was performed with ethanol and DCM, respectively. The product was further dried at 70 ºC ($\pm$1 °C) under vacuum. The steps for the synthesis of Cu(II)-hybrid is depicted in Scheme 1.

Catalytic evaluation

The catalytic activities of the as-synthesized Cu(II)-hybrid were evaluated by oxidative degradation of aqueous solution of RB5 and oxidation of organic substrates, i.e., tetralin, cycloalkane, and cycloalcohols.

Batch reaction procedure for dye degradation

Dye degradation experiment was performed by catalyzing aqueous solution of reactive black 5 (RB5) dye. A 500-mL solution of RB5 (45 ppm)
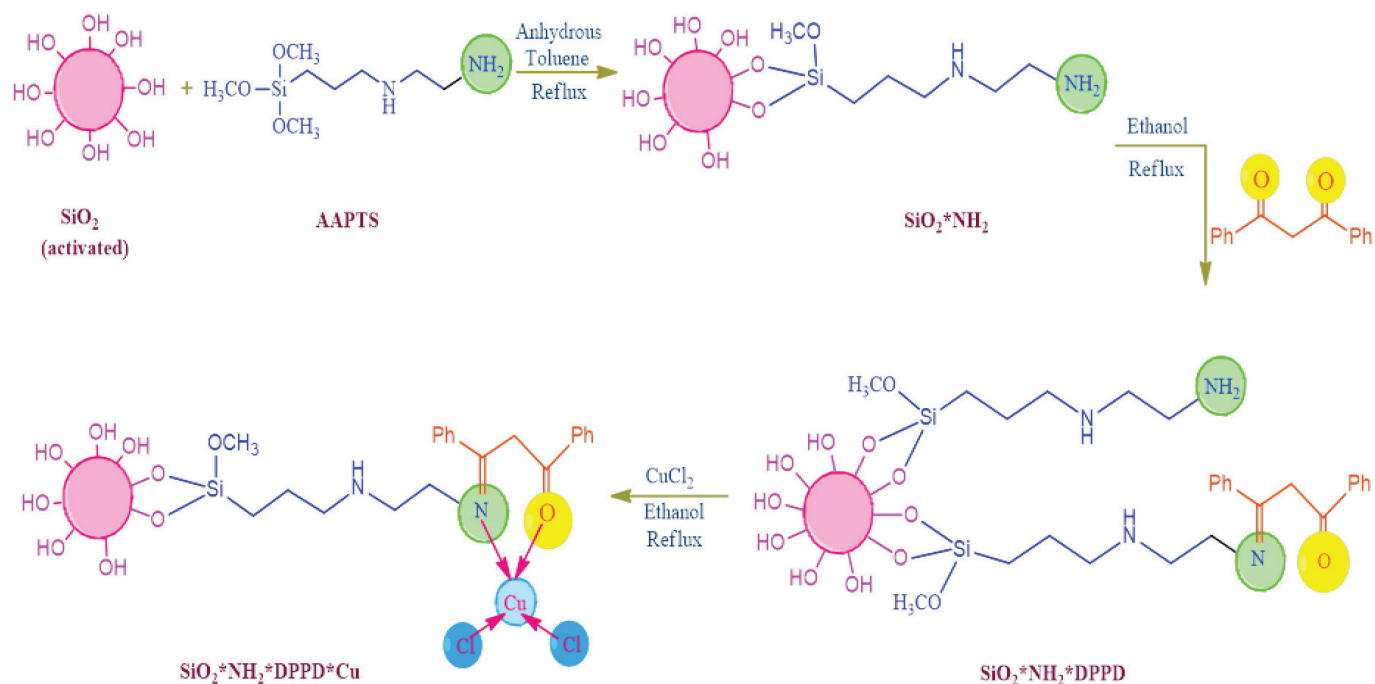
S c h e m e 1 – *Steps for the synthesis of Cu (II)-hybrid*

was prepared in Milli-Q water. The experiment was executed by mixing 25 mL of RB5 dye solution and 2 mL of H_2O_2 (4.41 mM, 8.82 mM, 17.6 mM and 26.46 mM). Hybrid catalyst (0.2 g L^{-1}, 0.4 g L^{-1}, 0.6 g L^{-1}, 0.8 g L^{-1} and 1.0 g L^{-1}) was added to this solution. These experiments were conducted at 35 ± 1 ℃. One-factor-at-a-time optimization was performed resulting in the optimum concentration of hybrid catalyst of 0.8 g L^{-1}, and H_2O_2 concentration of 17.6 mM. Finally, with the optimum concentrations of the H_2O_2 (i.e., 17.6 mM), and catalyst (i.e., 0.8 g L^{-1}), experiments were also performed at (45 and 55) ± 1 ℃.

All batch reaction experiments were performed at 35 ± 1 ℃ while continuously stirring with a magnetic stirrer at the speed of 1200 rpm. Each time an aliquot (2 mL) was withdrawn from the reaction mixture and filtered. The solution was then tested for remaining concentration of RB5 by monitoring its characteristic peak at absorption maximum (λ_{max}) = 596 nm, which decreased as the reaction proceeded. Control experiments were also executed to observe the individual effect of H_2O_2 and catalysts. For this, degradation experiment was performed with H_2O_2 only, and another experiment with catalyst only, keeping other experimental conditions as before.

Dye degradation percentage was calculated using following formula:

$$\text{Dye degradation}\,(\%) = \left[(C_{RB5})_0 - (C_{RB5})_t \right) / (C_{RB5})_0 \right] \cdot 100\,\%$$

where, $(C_{RB5})_0$ and $(C_{RB5})_t$ are initial and time-dependent concentrations of dye solutions.

Batch reaction procedure for oxidation of organic substrates

For oxidation of organic substrates (i.e.; tetralin, cyclohexane, and cycloalcohols,), reaction was carried out by taking 5 mM substrate, 1 mL H_2O_2 (17.6 mM) as oxidant, acetonitrile (solvent), and 0.02 g catalyst in a 100-mL reaction vessel. The mixture was refluxed at 70 °C (±1 °C) for 4 h with continuous stirring by a magnetic stirrer at the speed of 1200 rpm. After 4 h, the mixture was diluted with Milli-Q water and products were extracted by DCM. The catalyst was separated and products were analyzed by GC-MS. The conditions for catalytic oxidation of organic substrates were initially optimized to obtain best procedure. The optimization was done in terms of various solvents (glacial acetic acid, dimethyl sulfoxide, dimethylformamide, and acetonitrile), different temperatures (40 ℃, 50 ℃, 60 ℃ and 70 ℃), and different catalyst amounts (0.01 g, 0.02 g and 0.03 g); keeping other parameters same as previously mentioned, i.e., 5 mM substrate (tetralin was chosen as reference substrate) and 1 mL H_2O_2 (17.6 mM).

Study of reusability and stability of the catalyst

For performing reusability tests, the catalyst from previous experiment was washed with ethanol several times, and dried at 70 °C (±1 °C) in an oven. The reusability of the catalyst was investigated by degrading fresh solution of RB5 and oxidizing tetralin under best reaction conditions. The procedure for the catalytic study was the same as earlier.

The stability of catalysts was inspected by observing the leaching content of metal ions. For executing the leaching experiment, same model reaction for dye degradation experiment (17.6 mM H_2O_2, 0.8 g L^{-1} catalyst and 35±1 °C temperature) was performed for 30 minutes. The heterogeneous catalysts were then removed by filtration. The filtrates were allowed to react further for 60 minutes, and examined for dye degradation percentage.

The stability of the catalyst was also checked by analyzing the fresh and used hybrid through FTIR and SEM analyses. For this, the hybrid used in the dye degradation experiment was separated through filtration, washed several times with ethanol, and dried at 70 °C (±1 °C) in an oven.

Results and discussion

Characterization of the catalyst

FT-IR spectra

FT-IR spectra of silica based hybrid materials are illustrated in Fig. 1. FT-IR spectrum of SiO_2 (Fig. 1a) exhibited its distinct peaks at 3442 cm^{-1} and 1639 cm^{-1} due to surface silanol (Si–OH) stretching and bending vibrations, respectively. The band at 1091 cm^{-1} was due to asymmetric and that at 795 cm^{-1} was due to symmetric vibrations of Si–O–Si bond; and the band at 461 cm^{-1} was attributed to Si–O–Si bending vibrations. In the spectrum of SiO_2*NH_2 (Fig. 1b), some new peaks appeared. The bands at 2905 cm^{-1} and 2851 cm^{-1} were

attributed to the vibrations of C–H stretch and 1490 cm^{-1} to bending vibrations of C–H bond. The characteristic band in the region of 3000–3300 cm^{-1} for NH_2 stretching vibration was not clearly resolved in the FT-IR spectrum of the organo-functionalized silica gel. However, the band in the region of 3400–3500 cm^{-1} was due to O–H stretching vibration and exhibited deformation which may be assigned to unresolved N–H stretching vibration of SiO_2*NH_2. The presence of NH_2 group in the grafted SiO_2*NH_2 was further evidenced by an additional band at 1551 cm^{-1} assigned to of NH_2 bending vibration[28]. Grafting of AAPTS on the surface of silica was also confirmed through the shift observed in O–H stretching vibration, which shifted to lower wave number. Fig. 1c represents the FT-IR spectrum of Schiff's base formation on SiO_2*NH_2 grafted moiety. In the spectrum of SiO_2*NH_2*DPPD, new peak at 1668 cm^{-1} was observed, which characterized C=N stretching[29] and confirmed the formation of Schiff base as a result of reacting SiO_2*NH_2 and DPPD. Appearance of less intense bands at 1400–1500 cm^{-1} was attributed to aromatic rings stretching vibrations of DPPD. An additional band at 1728 cm^{-1} observed due to presence of C=O group, indicating that one of the C=O groups of DPPD did not participate in the Schiff base reaction. On metalation with copper(II) chloride, the C=N (1668 cm^{-1}) and C=O (1728 cm^{-1}) vibrations were shifted to 1636 and 1691 cm^{-1} respectively, i.e., to the lower wave number region, therefore confirming the coordination of metal ions through these groups (Fig. 1d). Further, the newly observed bands at 442 and 605 cm^{-1}
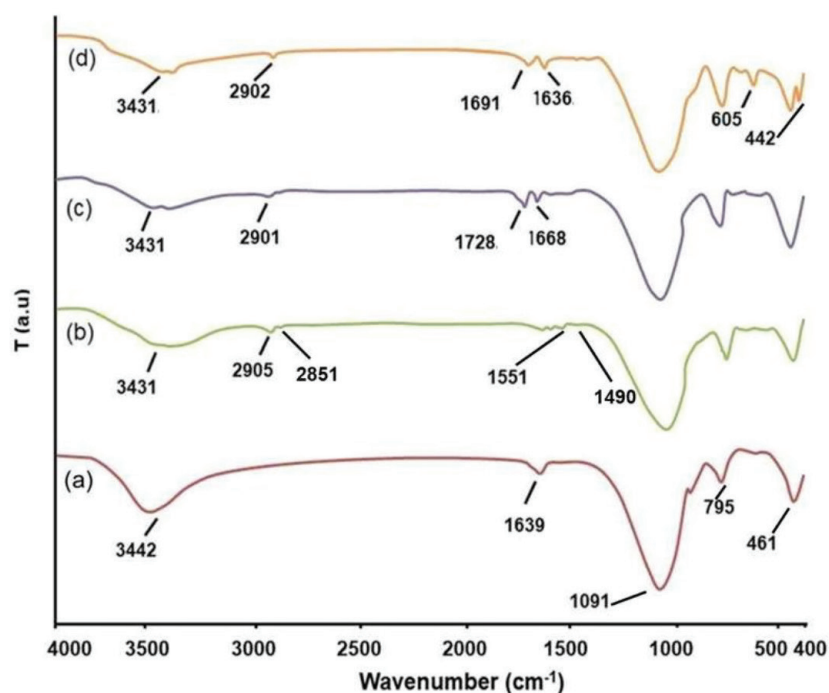

F i g . 1 – *Comparative FT-IR spectra for (a) SiO_2, (b) SiO_2*NH_2, (c) SiO_2*NH_2*DPPD, and (d) $SiO_2*NH_2*DPPD*Cu$*

might be assigned to stretching vibrations of Cu–N and Cu–O bonds, respectively[30]. This also supported the assumption that copper metal was coordinated with nitrogen of imine group and oxygen of C=O group of DPPD. The Metal–Cl vibrations generally occurred below 400 cm^{-1} and therefore could not be found in the spectrum.

Diffuse reflectance UV-Visible (DRUV-Vis) spectroscopy

Existence of organic functional groups in the synthesized materials was also confirmed through DRUV-Vis spectra, which are shown in Fig. 2. The electronic absorption spectrum of SiO_2 showed no absorption in the range of 200–800 nm, while that of SiO_2*NH_2 exhibited a band below 300 nm, which might be due to n-σ* transition of non-bonded electrons of NH_2 (Fig. 2b). After Schiff's base formation of grafted aminopropyl silica by DPPD, a band was observed around 250 nm in the UV-visible spectrum of SiO_2*NH_2*DPPD, which could be a result of π-π* electronic transition of phenyl ring. Absorbance peak near 360 nm might be assigned to n-π* transition of C=N non-bonded electrons, confirming the grafting of DPPD to the aminopropylsilica (Fig. 2c). The spectrum of Cu(II) metalated hybrid (Fig. 2d) also exhibited the n-π* and π-π* transition peaks, but they were shifted to higher wavelength suggesting the coordination of ligands to the Cu(II) ion. The low intensity band around 600 nm in the electronic spectrum of Cu(II)-hybrid (Fig. 2 inset) was assigned to $^2B_{1g} \rightarrow ^2A_{1g}$ transition, characteristic of square planar geometry[31].

Solid state ^{13}C CPMAS NMR spectroscopy

Functionalization of silica surface with AAPTS and formation of Schiff base was confirmed by Solid state ^{13}C NMR spectra (Fig. 3a). The peak at 9.861 ppm was assigned to the most shielded carbon atom (C1) due to its attachment with silicon atom. Peak at 23.016 ppm was due to –CH_2– group (C2), and those at 36.632 ppm (C3) and 38.714 ppm (C4) were designated to carbon atoms bound to –NH– group. Signal at 45.788 ppm was due to the carbon atom (C5) attached to amino group. Peak at 50.896 ppm was attributed to unsubstituted methoxy group[32]. Presence of these peaks confirmed that AAPTS had been successfully grafted on silica surface.

In the SiO_2*NH_2*DPPD spectrum, fourteen well resolved peaks were obtained (Fig. 3b). Signals at δ = 11.041, 22.406, 36.141, 39.327, and 52.059 ppm were assigned to C1, C2, C3, C4, and C7 respectively. N–CH_2 peak shifted to 57.699 ppm (C6) on Schiff's base formation, while the signal at 45.416 ppm (C5) was assigned to unreacted (free) –N–CH_2 group. Signal at 168.194 ppm was due to C=N group, which further supported the Schiff's base formation. Peak at δ = 186.652 ppm was attributed to C=O group, thereby indicating the non-involvement of one carbonyl group in the Schiff base reaction. C-9 gave the signal at 29.926 ppm. Peaks at 134.780 and 140.506 ppm were assigned to aromatic carbon atoms of phenyl rings attached to carbonyl group and imine group, respectively. Peaks at 128.628 and 122.646 ppm were due to remaining phenyl carbon atoms (C-a to C-f),
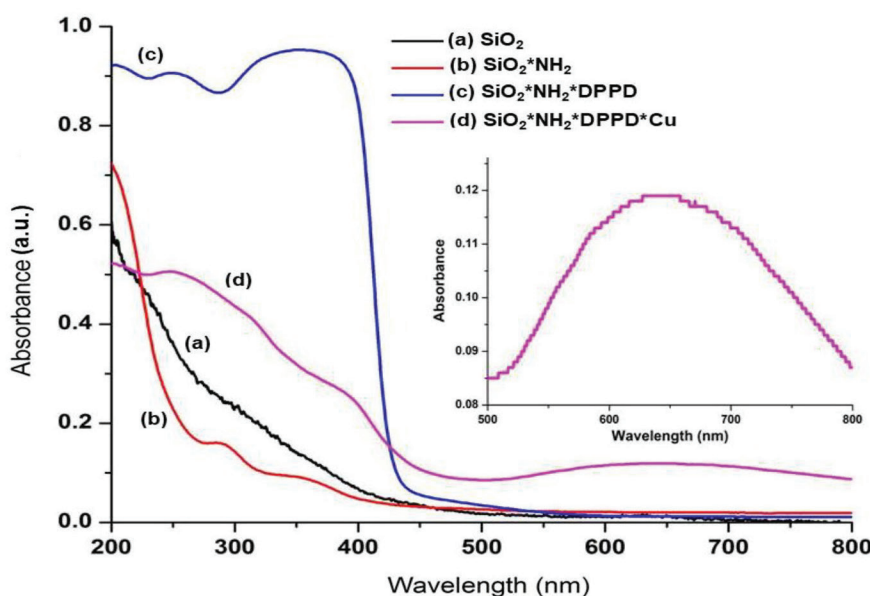

F i g . 2 – *DRUV-Visible spectra of (a) SiO_2 gel, (b) SiO_2*NH_2, (c) SiO_2*NH_2*DPPD, (d) $SiO_2*NH_2*DPPD*Cu$. The inset shows the spectrum of $SiO_2*NH_2*DPPD*Cu$ in the range of 500–800 nm.*
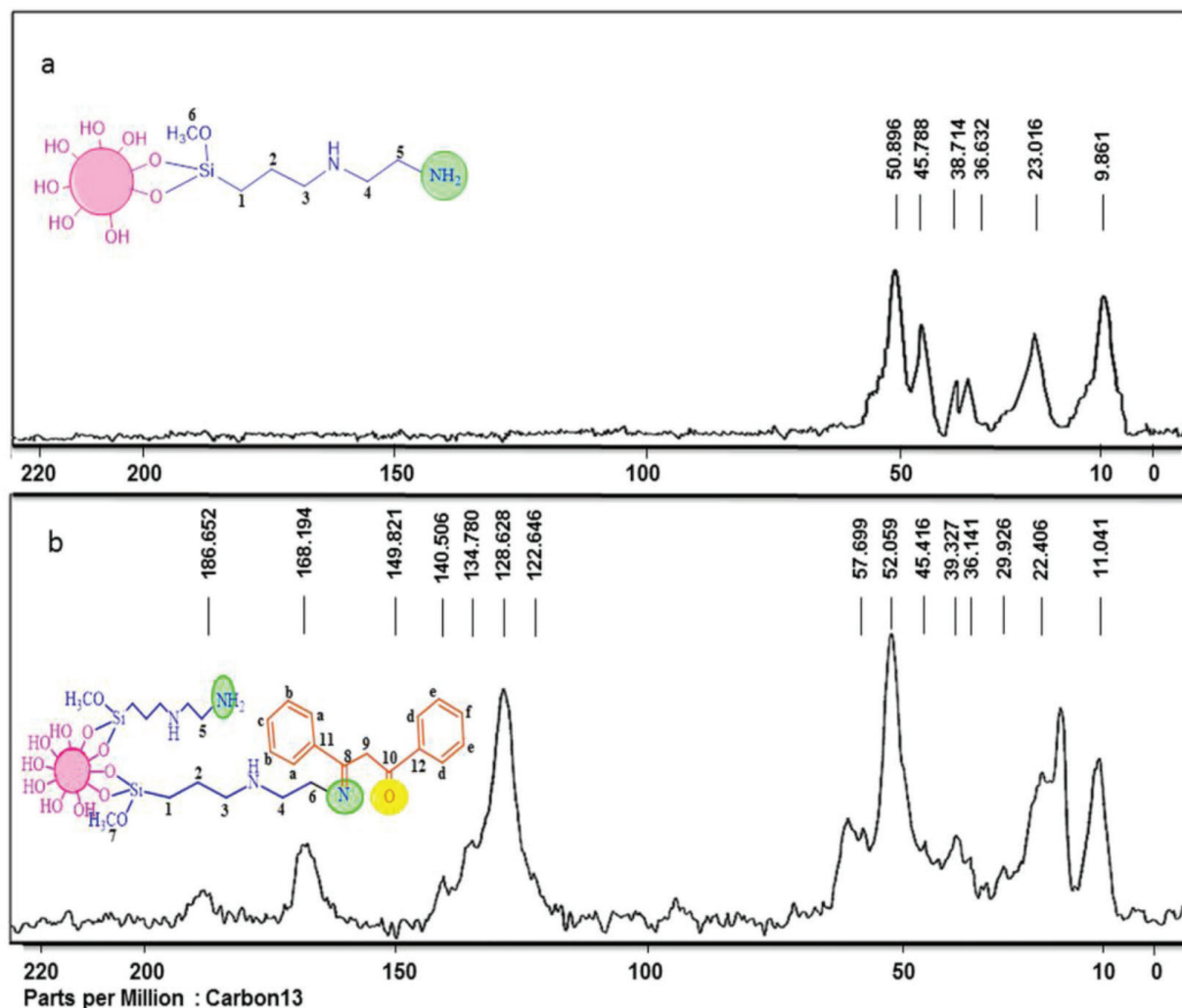
F i g . 3 – *Solid state ^{13}C NMR spectra of (a) SiO_2*NH_2, (b) SiO_2*NH_2*DPPD*

which should have been resolved into six peaks but resolution of these peaks were not achieved in solid state NMR spectrum.

Powder-XRD

Powder XRD analysis of all the relevant materials obtained after each step is exemplified in Fig. 4. A broad peak around $2\theta = 22°$ had been observed in the XRD pattern of SiO_2, a distinguishing feature of topological structure of silica[7,27]. This distinctive peak was also observed in the graph of the rest of the synthesized compounds, Fig. S1 (Supplementary Information).

SEM

SEM micrographs of SiO_2 gel and its modified forms are delineated in Fig. S2 (Supplementary Information). As seen from SEM micrograph, the ungrafted silica (SiO_2) particles had irregular shape, which they retained after modification. It was also observed that, after successive modifications, sur-

face became slightly rough, which might have been due to the attachment of organic groups.

ICP-AES (Inductively coupled plasma atomic emission spectroscopy) and EDX (energy dispersive X-ray) analysis

EDX analysis of the Cu(II)-hybrid is depicted in Fig. 4 illustrating the presence of all expected elements, thereby indicating the formation of Cu(II)-hybrid. To support the presence of copper and find its coordinated amount, ICP-AES investigation of the hybrid catalyst was executed. In the analysis, weight % of Cu was found to be 2.352 % and is almost similar to the EDX result which further supported the proposed structure for the hybrid. Also, as per EDX analysis, 0.804 mmol AAPTS, 0.458 mmol Cu, and 0.625 mmol of Cl are bonded to one gram of the sample.

Thermogravimetric analysis (TGA)

Thermal behavior of the synthesized materials was investigated by TGA (Fig. 5). SiO_2 exhibited a
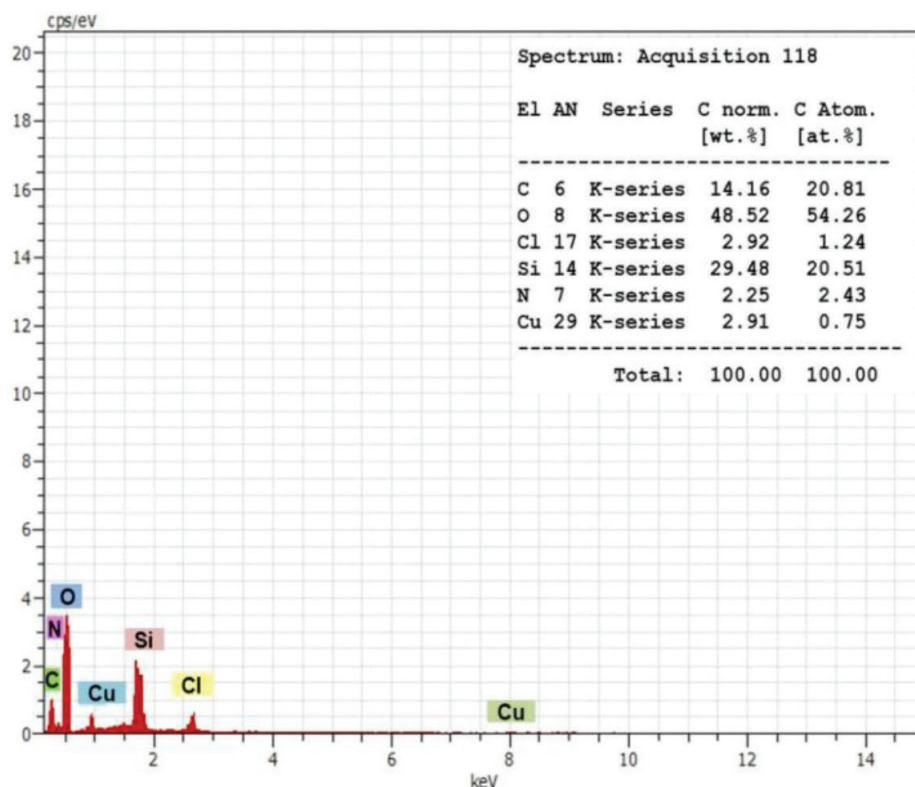
F i g . 4 – *EDX spectrum of SiO₂*NH₂*DPPD*Cu*

minor weight loss of approximately 5 % in the entire temperature scan (Fig. 5a). The weight loss in the range of 100–120 ºC might be attributed to the removal of physically adsorbed molecules of water, indicating the hydrophilic nature of silica matrix[33]. The TGA curve of SiO_2*NH_2 (Fig. 5b) showed a total weight loss of 15 %. The first decomposition peak (100–130 ºC) was attributed to the loss of ad-
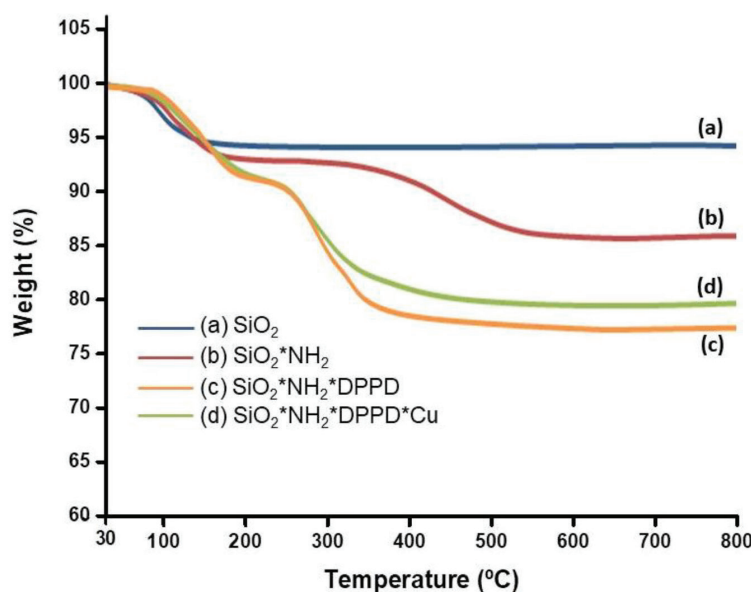
sorbed water molecules, and the second one (390–510 ºC) to the decomposition of chemically bonded AAPTS, revealing therefore, the grafting of approximately 0.99 mmol AAPTS per gram of SiO_2. Thermogram of SiO_2*NH_2*DPPD (Fig. 5c) illustrated a higher total weight loss of 23 % where the decomposition peak at 250–340 ºC could be due to the loss of DPPD molecules. The TGA analysis showed the loading of approximate 0.53 mmol DPPD/g SiO_2*NH_2. Cu(II)-hybrid ($SiO_2*NH_2*DPPD*Cu$) showed a weight loss of approximately 21 % (Fig. 5d). Since the metal ion on heating in the presence of oxygen from the organic moiety is converted to metal oxide and remains present on the solid matrix, the overall % weight loss decreases slightly, i.e., from 23 to 21. The mean degradation temperature for the thermogram had shifted to higher side, which could be attributed to the silica silane-Schiff's base stabilization by metalation (Fig. 5d). The weight loss observed from the thermogram of Cu(II)-hybrid revealed an approximate attachment of 0.346 mmol Cu/g SiO_2*NH_2*DPPD, which is close to EDX result, i.e., 0.458 mmol Cu per gram of the sample.

Electron paramagnetic resonance (EPR) spectrum

The powder X-band EPR spectrum of Cu(II)-hybrid at room temperature is shown in Fig. S3 (Supplementary Information). The EPR spectrum is typical of a normal axial monomeric Cu

F i g . 5 – *TG curves of (a) SiO₂ gel, (b) SiO₂*NH₂, (c) SiO₂*-NH₂*DPPD, (d) SiO₂*NH₂*DPPD*Cu*

species with $d_{x^2-y^2}$ as ground state. On comparing the calculated g factors, it was found that g factors were in order of g_{II} (2.2881) > $g_{\perp}$ (2.0596) > 2.0023, indicating the presence of unpaired electron in $d_{x^2-y^2}$ orbital[7]. This suggested the geometry of the compound to be square planar. Generally, the perpendicular feature of the spectrum comprised of a series of closely spaced, overlapping lines, appearing as a result of coupling of unpaired electron with copper nucleus, which could not be resolved at room temperature. From the spin Hamiltonian parameters, it appeared that the system was very likely to be square planar. Square planar geometry of the Cu(II)-hybrid is also in agreement with the DRUV-Vis spectrum.

It is reported that g_{II} > 2.3 represents ionic environment, and g_{II} < 2.3 indicates considerable covalent character in the metal-ligand bonding[34]. The g_{II} value obtained from the spectrum of Cu(II)-hybrid was less than 2.3, thereby suggesting the possible covalent character of the Cu-ligand bond. The g_{av} value was calculated from $g_{av}^2 = (g_{II}^2 + 2 g_{\perp}^2)/3$, giving the value of 2.13 for the hybrid. Its deviation from the g-value of free electron (2.0023) might be due to covalent character in the metal-ligand bond[35]. The exchange coupling factor (G) was calculated using following formula[7]:

$$G = \left[(g_{II} - 2)/(g_{\perp} - 2) \right]$$

If G > 4, it denotes parallel aligned or slightly misaligned local axes with negligible exchange coupling; and if G < 4, it symbolizes remarkably misaligned local axes with considerable exchange coupling[7]. Here, G value was calculated as 4.83,
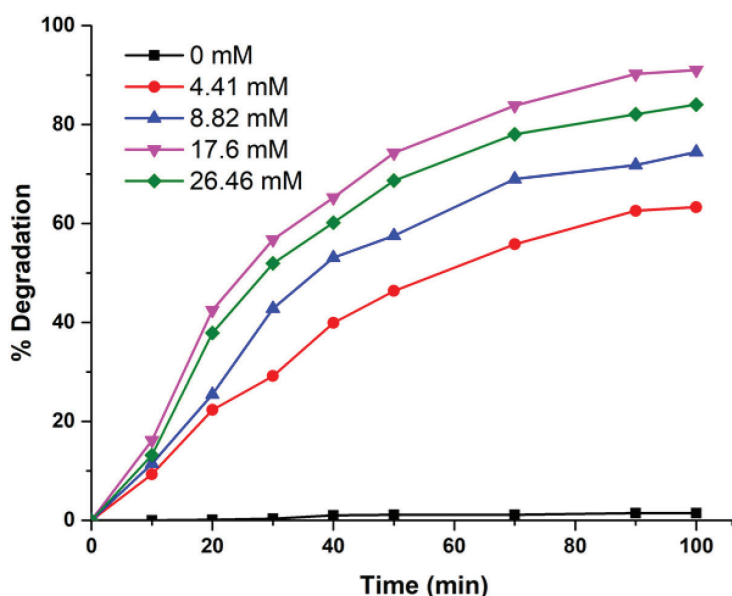
thus, having no copper-copper exchange interactions. Thus, it may be concluded that the present Cu(II)-hybrid exhibited significant covalent character with no Cu(II) – Cu(II) exchange. Additionally, small splitting in the perpendicular signal may be due to difference in bond length of M–O, M–N and M–Cl ligands.

Catalytic evaluation

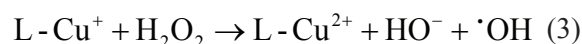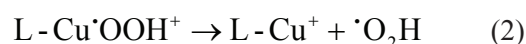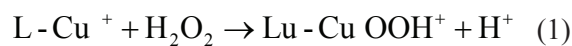### Oxidative degradation of RB5

Optimization of reaction conditions

The process parameters were optimized in terms of effect of H_2O_2 concentration, catalyst concentration and reaction temperature to achieve a given output with best inputs.
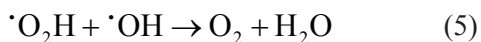
Effect of H_2O_2 concentration

Effect of H_2O_2 concentration was investigated by varying its concentration from 0 to 26.46 mM, while maintaining other parameters constant, i.e., catalyst concentration at 0.8 g L^{-1} and temperature at 35 ± 1 ºC. It was observed that dye degradation percentage at (0, 4.41, 8.82, 17.6, and 26.46) mM H_2O_2 was 1 %, 63 %, 72 %, 91 %, and 84 %, respectively (Fig. 6). Thus, degradation of RB5 showed acceleration up to 17.6 mM, but further increase in concentration of H_2O_2 decreased the degradation percentage. The enhancement in the degradation at beginning of reaction may have been due to increased generation of beneficial hydroxyl radicals ($\cdot$OH), which acted as strong oxidizing agents and reacted with dyes, leading to their degradation[36].

Several studies have reported Cu-mediated homogeneous catalytic decomposition of hydrogen peroxide[37–39]. Mechanism for H_2O_2 decomposition can be represented by a Fenton-like reaction, as given by Lin *et al.*[40] (Eq.1–3), where L symbolizes the ligand used in their system.

$$L\text{-}Cu^+ + H_2O_2 \rightarrow Lu\text{-}Cu\,OOH^+ + H^+ \quad (1)$$

$$L\text{-}Cu\,\!^{\cdot}OOH^+ \rightarrow L\text{-}Cu^+ + \,^{\cdot}O_2H \quad (2)$$

$$L\text{-}Cu^+ + H_2O_2 \rightarrow L\text{-}Cu^{2+} + HO^- + \,^{\cdot}OH \quad (3)$$

This could be a possible mechanism for H_2O_2 decomposition in the present system.

Further, decrease in efficiency upon increasing H_2O_2 concentration might be due to scavenging of useful $\cdot$OH radicals and generation of hyperoxyl radicals ($\cdot O_2H$), which are quite less reactive with no capability of degrading organic molecules. These $\cdot O_2H$ radicals further react with $\cdot$OH radical to form oxygen and water[41].

F i g . 6 – *Effect of H_2O_2 concentration on degradation of RB5 (RB5 concentration = 45 ppm, catalyst concentration = 0.8 g L^{-1}, temperature = 35 ± 1 ºC)*

$$H_2O_2 + {}^{\cdot}OH \rightarrow {}^{\cdot}O_2H + H_2O \qquad (4)$$

$${}^{\cdot}O_2H + {}^{\cdot}OH \rightarrow O_2 + H_2O \qquad (5)$$

As oxidation potential of ${}^{\cdot}O_2H$ (1.78 V) is less than that of ${}^{\cdot}OH$, self-scavenging cannot promote degradation of dye molecules[42]. Thus, effective dosage of H_2O_2 was taken as 17.6 mM for further studies.

A very small amount of H_2O_2 was required to initiate the degradation process, and the dye degraded to very low extent in the absence of H_2O_2. In the presence of catalyst, the dye degraded to high extent, and therefore, it was very important to investigate whether the decline in the concentration of dye had occurred by adsorption of dye molecules on the surface of catalyst or by degradation through oxidative catalysis or by both. For this, a batch reaction was operated by taking 25 mL RB5 solution (45 ppm) and synthesized catalyst (0.8 g L^{-1}). The suspension was stirred for 4 h at 35 ± 1 ºC. The decrease in λ_{max} (596 nm) was calculated by observations from UV-Vis spectra, and it was found to be only 3 %, Fig. S4 (Supplementary Information). Thus, it can be concluded that RB5 removal was not by adsorption but due to oxidative catalytic degradation by the Cu (II)-hybrid.

Effect of catalyst concentration

To examine the effect of catalyst concentration, experiments were carried out with different quantities of catalyst (0.2, 0.4, 0.6, 0.8, and 1.0) g L^{-1}; keeping other parameters same, i.e., H_2O_2 concentration at 17.6 mM and temperature at 35 ± 1 ºC.

F i g . 8 – *Effect of temperature on degradation of RB5 (RB5 concentration = 45 ppm, H_2O_2 concentration = 17.6 mM, catalyst concentration = 0.8 g L^{-1})*

Effect of catalyst concentration on RB5 degradation is presented in Fig. 7, from which it can be seen that degradation efficiency in the absence of catalyst was only 7 % even after 100 minutes of reaction process. This efficiency increased to 52 %, 68 %, 73 %, and 91 % when catalyst was taken as 0.2 g L^{-1}, 0.4 g L^{-1}, 0.6 g L^{-1} and 0.8 g L^{-1}, respectively. This might be due to increase in more active sites for H_2O_2 molecules on catalyst surface. However, increasing the catalyst amount to 1.0 g L^{-1} did not improve the degradation efficiency significantly; possible reason may be that the increased amount of catalyst did not cause reaction between H_2O_2 molecules and active center (i.e., copper). Thus, 0.8 g L^{-1} was taken as best catalyst concentration.

The role of catalyst in the degradation of RB5 was also observed by performing the batch experiment in the presence of unmodified silica gel instead of catalyst. Here, degradation was only 10 % even after 3 h, Fig. S5 (Supplementary Information). This result proved that the catalyst showed high activity towards RB5 degradation.

Effect of temperature

RB5 degradation was significantly influenced by the change in temperature and percentage degradation of dye with time at different temperatures (35, 45, 55 ºC) ± 1 ºC, as shown in Fig. 8. It was observed that dye degradation percentage increased with time. Also observed was that degradation of RB5 dye increased with temperature, as expected.
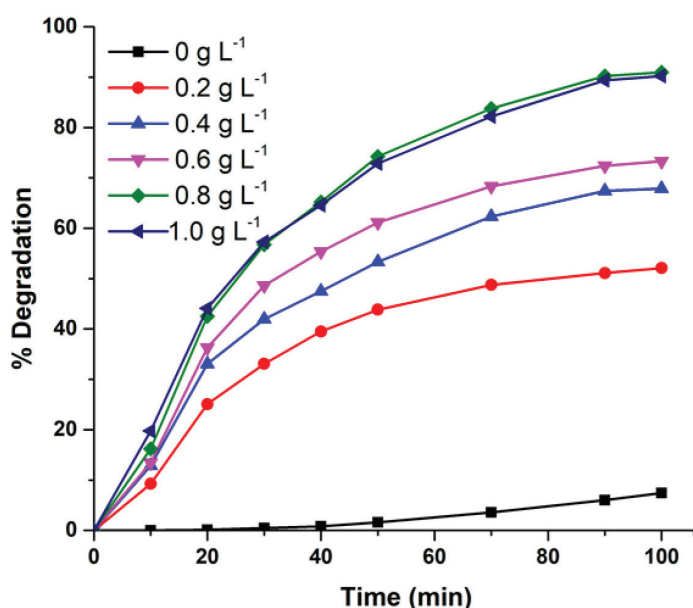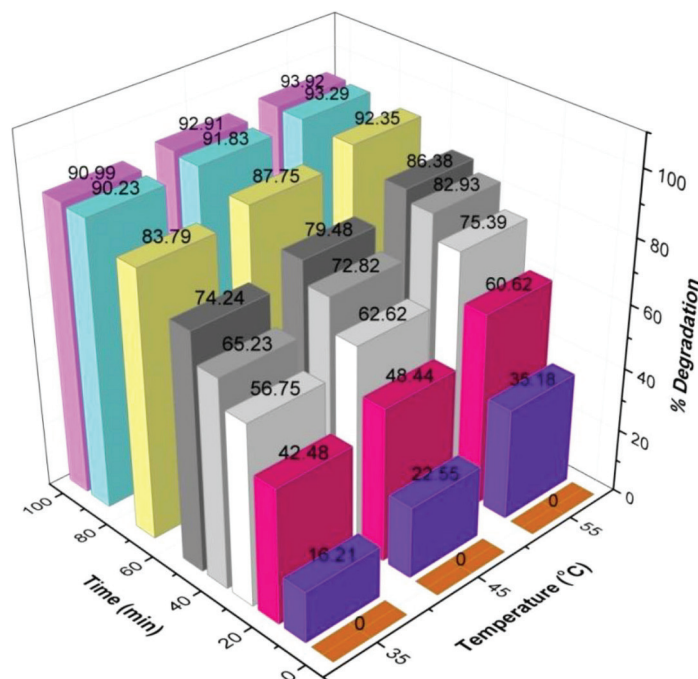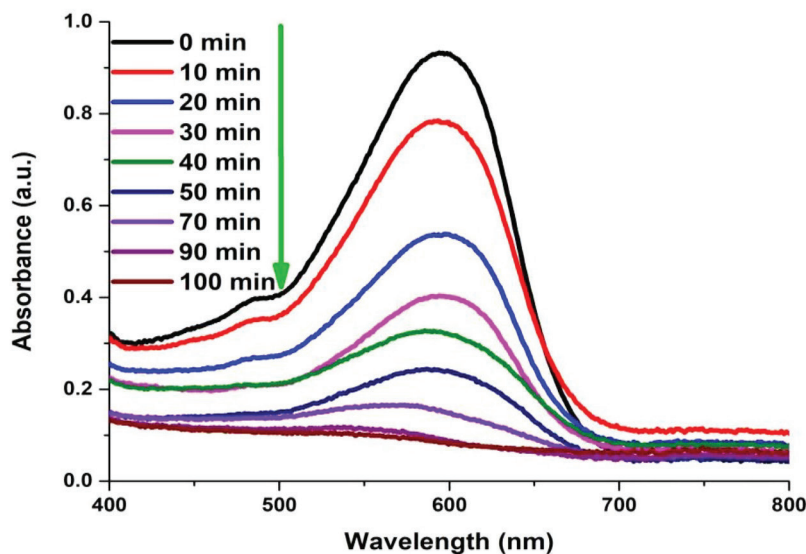

F i g . 7 – *Effect of catalyst concentration on degradation of RB5 (RB5 concentration = 45 ppm, H_2O_2 concentration = 17.6 mM, temperature = 35 ± 1 ºC)*

F i g . 9 – *Time-dependent UV-Vis spectrum of RB5 aqueous solution (45 ppm) in presence of H₂O₂ (17.6 mM) and catalyst (0.8 g L⁻¹) at 35 ± 1 °C*

The reason for this being that, with the rise in temperature, oxidation proceeds at a faster rate[43]. This increase in oxidation could be attributed to the high heat energy which enhanced the collision between H_2O_2 and active sites of Cu(II)-hybrid, thereby promoting the generation of ·OH radicals[44]. These ·OH radicals collide with RB5 molecules, thereby oxidizing them. As more ·OH radicals are generated by high temperature, thus the dye is more degraded. However, we operated all the reactions at 35 °C, as high temperature requires more energy and increased process cost. Thus, 35 °C was chosen as best temperature for the degradation studies. In addition, at higher temperature (45 °C), the catalytic activity of hybrid was not affected, implying that no possible leaching or decomposition of the catalyst occurred in the reaction environment.

On the basis of above studies, the absorbance of RB5 dye solution with time at the best reaction conditions, i.e., 17.6 mM H_2O_2 concentration, 0.8 g L⁻¹ catalyst concentration, and 35 °C temperature is shown in Fig. 9. As seen from the figure, the absorbance of dye decreases with time which indicates decrease in dye concentration with time. The concentration of RB5 corresponding to particular absorbance was calculated through the calibration curve obtained by plotting absorbance versus known concentrations of dye, and is presented in Fig. S6 (Supplementary Information).

Role of scavenger on dye degradation

To support the proposed mechanism of RB5 degradation involving ·OH radicals, dye degradation process was performed in the presence of a strong hydroxyl radical scavenger, isopropyl alcohol. Batch reaction was performed as described previously. However, in this case, 2.5 mL of 2-propanol (0.1 M) was also added to the reaction mixture. Effect of scavenger on dye degradation with time is presented in Fig. S7 (Supplementary Information). It was observed that dye degradation decreased from 91 % (without scavenger) to 68 % (in the presence of scavenger), thereby confirming the hydroxyl radicals as the active species during dye degradation process.

Kinetic analysis

On the basis of experimental analysis and reported literature[45], it is proposed that the degradation reaction of RB5 with hydrogen peroxide (H_2O_2) in presence of hybrid catalyst follows the following stoichiometric representation:

$$RB5 + H_2O_2 \rightarrow P + CO_2 \tag{6}$$
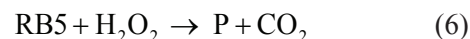
where P symbolizes oxidized products after RB5 degradation. The other product formed during the degradation reaction was carbon dioxide. To obtain the kinetics of the reaction, concentration/absorbance of RB5 was monitored; however, the formation of carbon dioxide during the process was confirmed by lime water test, which supported the above proposed mechanism.

On the basis of kinetic analysis, the proposed rate of disappearance of RB5 is given below:

$$(-r_{RB5}) = k\left(C_{RB5}\right)\left(C_{H_2O_2}\right) \tag{7}$$

where, C_{RB5} is concentration of RB5, and $C_{H_2O_2}$ is that of H_2O_2.

Further, to verify the proposed kinetics and evaluate the rate constant in Eq. 7, experiments were performed with best concentration of H_2O_2

(17.6 mM) for maximum degradation of RB5. The results were plotted to obtain the best fitted curve, and it was observed that the reaction followed pseudo-first order kinetics. Since the best concentration of H_2O_2 during the experiment was in excess, its concentration was nearly constant during the reaction. The resulting reaction kinetics is given below:

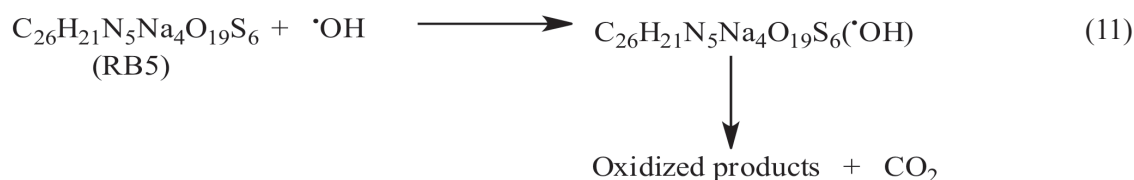$$(-r_{RB5}) = k_{obs}(C_{RB5}) \qquad (8)$$

where, $k_{obsk} = k(C_{H_2O_2})$.

In the above equation, k_{obs} is pseudo first order rate constant, and k is the rate constant of the actual second order reaction. The system used in this investigation is a liquid-liquid system, thus, the volume of the reaction mixture was considered as constant. For this system, following correlation represents the relationship between RB5 concentration and time:

$$-\ln\left[(C_{RB5})_t / (C_{RB5})_0\right] = k_{obs} \cdot t \qquad (9)$$

where, $(C_{RB5})_0$ and $(C_{RB5})_t$ are the initial concentration and time-dependent concentration of RB5, respectively. To further verify the kinetics, $-\ln[(C_{RB5})_t/(C_{RB5})_0] = k_{obs} \cdot t$ obtained at 35 ºC was plotted against time (t), as shown in Fig. S8 (Supplementary Information); the plotted data points lie on straight line with regression coefficient R^2 value equal to 0.993.

This confirmed that the reaction was of pseudo first-order and the observed value of the rate constant (k_{obs}) was 0.026 min^{-1}. In addition, average calculated value of the second order reaction rate constant (k) was 1.42 L mol^{-1} min^{-1} at 35 ºC.

Experiments were also conducted at two more temperatures, i.e., 45 ºC and 55 ºC to obtain the activation energy of the reaction. $-\ln[(C_{RB5})_t/(C_{RB5})_0]$ vs time graph at these temperatures show same trend as obtained at 35 ºC. The rate constants at two aforementioned temperatures were 1.54 L mol^{-1}min^{-1} and 1.59 L mol^{-1} min^{-1}, respectively. In addition, the calculated values of frequency factor and activation energy of the reactions were 8.73 and 4632 J mol^{-1} K^{-1}. The final rate expression for degradation of RB5 is as follows:

$$(-r_{RB5}) = 8.73\, e^{-\frac{4632}{RT}} C_{RB5} C_{H_2O_2} \qquad (10)$$
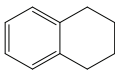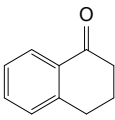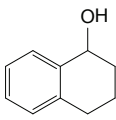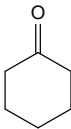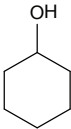
$-\ln[(C_{RB5})_t/(C_{RB5})_0]$ vs time graph (at 35 ºC) was also plotted for different concentrations of H_2O_2 and catalyst, and it followed the same trend as obtained in Fig. S8 (Supplementary Information).

Plausible mechanism for RB5 degradation

The mechanism suggests that H_2O_2 molecules are firstly activated by the Cu(II) catalyst to generate highly active ·OH radicals. The hydroxyl radicals have the capability of attacking organic 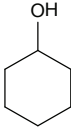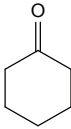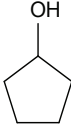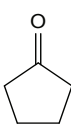substrates, resulting in the chemical decomposition of these substrates by H abstraction and addition to C=C unsaturated bonds[41]. Thus, the generated ·OH radicals combined with RB5, and converted it into dye-radical adduct. This intermediate product later on converted into oxidized products[45] and carbon dioxide. The mechanism for the degradation of RB5 is shown in eq. 11.

$$\underset{\text{(RB5)}}{C_{26}H_{21}N_5Na_4O_{19}S_6} + \cdot OH \longrightarrow C_{26}H_{21}N_5Na_4O_{19}S_6(\cdot OH) \qquad (11)$$

$$\downarrow$$

$$\text{Oxidized products} + CO_2$$

Oxidation of organic substrates

Conditions for oxidizing organic substrates (tetralin, cyclohexane, cyclohexanol and cyclopentanol) were optimized in terms of various solvents (viz., glacial acetic acid, dimethyl sulfoxide, dimethylformamide, and acetonitrile) and temperature variation (40, 50, 60, and 70) ºC (± 1 ºC) at 17.6 mM H_2O_2 and 0.02 g catalyst. Tetralin was taken as reference substrate. It was observed that maximum product yield was obtained in case of acetonitrile as compared to other solvents. Previous studies have also shown that acetonitrile is an effective and widely used solvent[7,46]. We also observed in our previous work[47] that acetonitrile was the best solvent in tetralin oxidation by polyoxometalate based catalyst. Therefore, other experiments were performed using acetonitrile as solvent. While observ-

ing temperature variation effect, it was noted that maximum yield was obtained at 70 ºC (± 1 ºC). Thus, the catalytic ability of the synthesized catalyst was evaluated through oxidation of all organic substrates in acetonitrile at 70 ºC (± 1 ºC) with 0.02 g catalyst; keeping H_2O_2 concentration at 17.6 mM. The oxidation products obtained after catalyzing aforementioned organic substrates at best reaction conditions were analyzed by GC-MS, and the graphs thus obtained are shown in Fig. S9–S16 (Supplementary Information). The results obtained by the oxidation of these organic substrates after 4 h are summarized in Table 1. The results show that organic substrates were readily oxidized into their respective products with good yield, and good selectivity was obtained for the value added industrial products.

Table 1 *Oxidation of cycloalkanes and cycloalcohols with H_2O_2 catalyzed by hybrid catalyst*

S. No.	Substrate	Product		Conversion (%)[a, b]		Selectivity (%)	
		A	B	A	B	A	B
1.	Tetralin	1-Tetralone	1-Tetralol	31.63	10.98	74.23	25.77
2.	Cyclohexane	Cyclohexanone	Cyclohexanol	30.84	10.25	75.05	24.95
3.	Cyclohexanol	Cyclohexanone	–	40.54	–	100	–
4.	Cyclopentanol	Cyclopentanone	–	38.44	–	100	–

(A) Ketone
(B) Alcohol
(a) Reaction conditions: Substrate (5 mM), H_2O_2 (17.6 mM), catalyst (0.02 g), CH_3CN (solvent), T = 70 ℃ (±1 ℃)
(b) Determined from GC analysis

Blank catalytic experiment, i.e., without catalyst, was also conducted for tetralin oxidation at the best reaction conditions, but negligible product yield was obtained. This showed the importance of synthesized catalyst in these conversions.

Among all the tested substrates, tetralin gave the highest percent conversion of 42.61 % into 1-tetralone (31.63 % yield) and 1-tetralol (10.98 % yield) with the selectivity of 74.23 % and 25.77 % for tetralone and tetralol, respectively. Cyclohexane showed the percent conversion of 41.09 % into cyclohexanone (30.84 % yield) and cyclohexanol (10.25 % yield) with the selectivity of 75.05 % and 24.95 %, respectively. Cyclohexanol gave the product (cyclohexanone) yield of 40.54 % with 100 % selectivity, and cyclopentanol gave the product (cyclopentanone) yield of 38.44 % with 100 % selectivity. Oxidation products obtained are of high industrial value. The advantage of using heterogeneous catalysts is their recyclability and simple workup process, which may lead to future industrial development process.

Reusability and stability of the catalyst

The reusability of the catalyst was tested for dye degradation and oxidation of tetralin. It was observed from the results that there was no substantial loss in the catalytic efficiency of the Cu(II)-hybrid. Percentage degradation of dye was 90.84 % and 90.35 % in the second and third catalytic cycle, respectively; slightly lower than first catalytic cycle, which gave 90.99 % dye degradation percentage.

The GC-MS graphs obtained for second and third catalytic cycle in the oxidation of tetralin are shown in Fig. S17–S20 (Supplementary Informa-
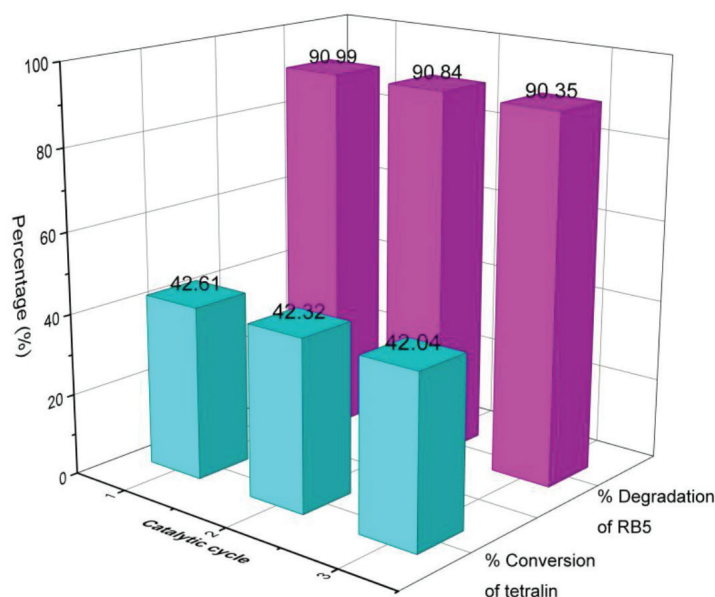
Fig. 10 – *Catalytic reusability of SiO₂*NH₂*DPPD*Cu*

tion). These results indicated that in the second and third catalytic cycle, there was no significant loss in the product yield of organic substrates. Conversion of tetralin was 42.32 % and 42.04 % in the second and third catalytic cycle, respectively, with the product selectivity of 74.64 % (tetralone) and 25.36 % (tetralol) in the second run, and 73.59 % (tetralone) and 26.41 % (tetralol) in the third run. The graphic representation for reusability of the catalyst for dye degradation and substrate conversion in its first, second, and third cycle is presented in Fig. 10.

Leaching experiment was also performed to observe the stability of hybrid material. The results obtained from the leaching experiments showed that there was no significant increase in degradation when catalyst was filtered from the reaction mixture after 30 minutes and filtrate (obtained during leaching experiment) was allowed to react for another 60 minutes. Time-dependent UV-Vis spectrum of RB5 aqueous solution for observing leaching of the metal ion from the hybrid material is shown in Fig. S21 (Supplementary Information). Previous studies have shown that Cu(II) ions have the tendency to degrade dyes[48,49], and hence, in our case, dye would have been degraded if leaching of metal ion had occurred. This supports that no substantial leaching of metal ions had occurred, and thereby corroborates that the synthesized catalyst was truly heterogeneous in nature. To observe the stability of the synthesized hybrid material, FT-IR and SEM analyses of reused hybrid were also performed. Surface morphologies of fresh and used catalyst were found almost the same, as seen in SEM images, Fig. S22 (Supplementary Information). Only some aggregation was observed on the surface of used catalyst.

FTIR spectra of fresh and recovered catalyst revealed no obvious change in the pattern, Fig. S23 (Supplementary Information). Thus, it can be concluded that Cu(II)-hybrid had not degraded during experiments.

Conclusions

Silica surface was modified with 3-(2-aminoethylamino) propyltrimethoxysilane and successfully reacted with 1,3-diphenyl-1,3-propanedione to yield Schiff's base. Copper(II) ion was then immobilized on the Schiff's base-modified silica gel, thereby synthesizing a novel Cu(II)-based inorganic-organic hybrid by following facile synthetic method. The hybrid was characterized by relevant spectral and surface analytical techniques, and used as an efficient heterogeneous catalyst for oxidative degradation of reactive black 5 dye with 91 % degradation and oxidation of some organic substrates, viz., tetralin, cyclohexane, cyclohexanol and cyclopentanol to obtain products of industrial importance. Conversion of tetralin, cyclohexane, cyclohexanol and cyclopentanol was 42.61 %, 41.09 %, 40.54 % and 38.44 %, respectively. Reaction kinetics for dye degradation was studied in detail, and was found to follow second order kinetics with rate constant equal to 1.42 L mol⁻¹ min⁻¹ at 35 ºC. Frequency factor and activation energy of the reaction were also calculated as 8.73 and 4632 J mol⁻¹ K⁻¹, respectively. The catalytic activities were studied in mild reaction conditions for an eco-friendly, green approach. Catalyst was easily recovered by filtration and washing, and used three times with almost no significant loss in its catalytic activity.

Supplementary Information

F i g . S 1 – *Powder XRD patterns of (a) SiO$_2$ gel, (b) SiO$_2$*NH$_2$, (c) SiO$_2$*NH$_2$*DPPD, (d) SiO$_2$*NH$_2$*DPPD*Cu*
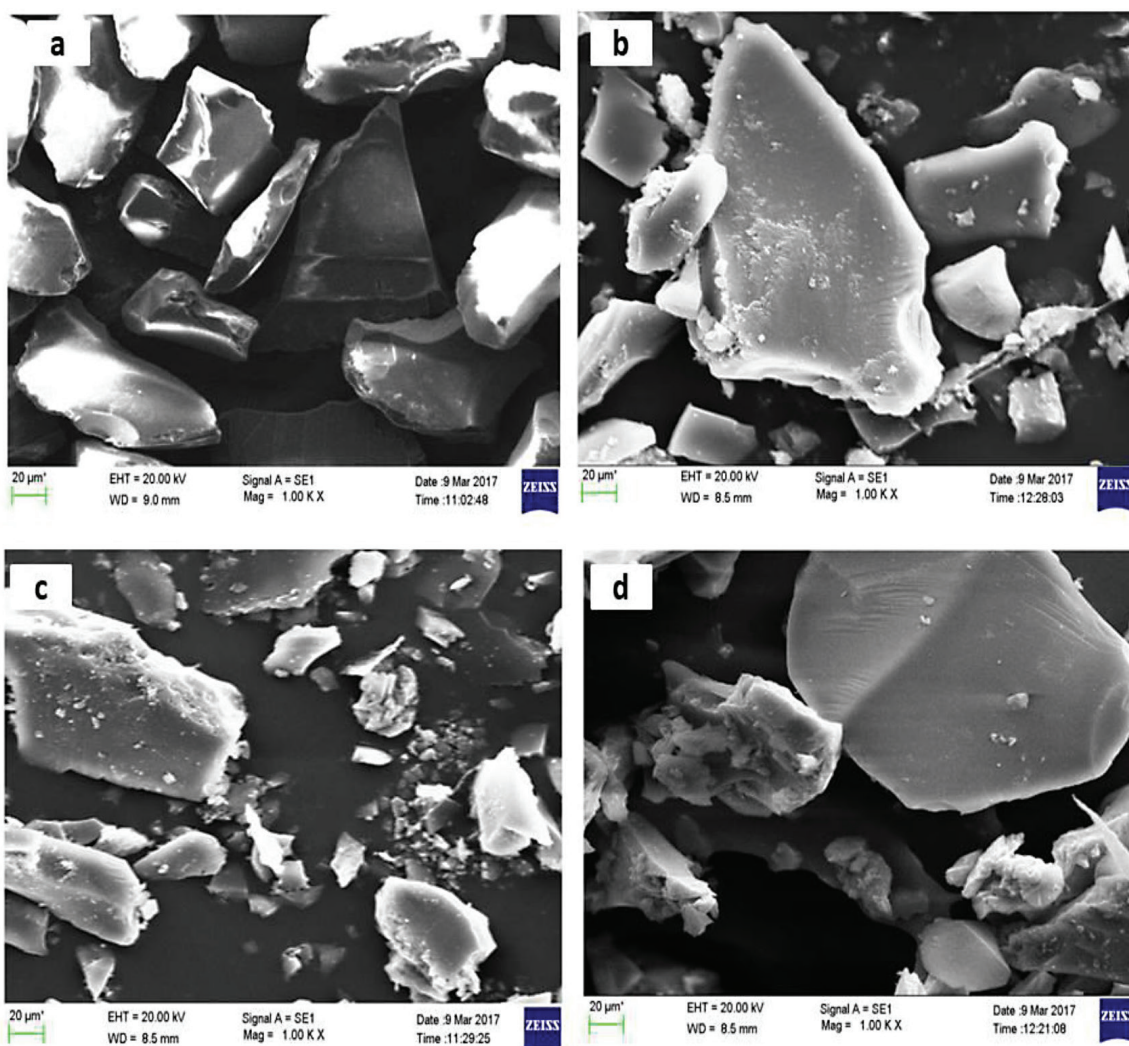
F i g . S 2 – *SEM images of (a) SiO$_2$ gel, (b) SiO$_2$*NH$_2$, (c) SiO$_2$*NH$_2$*DPPD, (d) SiO$_2$*NH$_2$*DPPD*Cu*
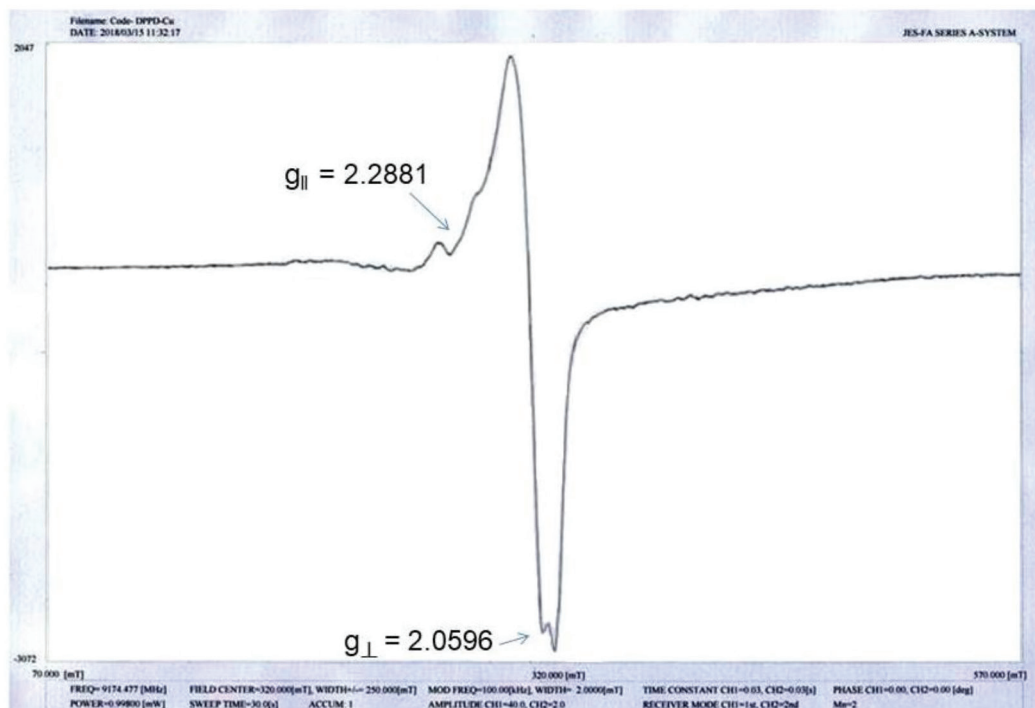
F i g . S 3 – *X-band EPR spectrum of SiO$_2$*NH$_2$*DPPD*Cu*

F i g . S 4 – *Time-dependent UV-Vis spectrum of RB5 aqueous solution in presence of catalyst only (4 hours study)*
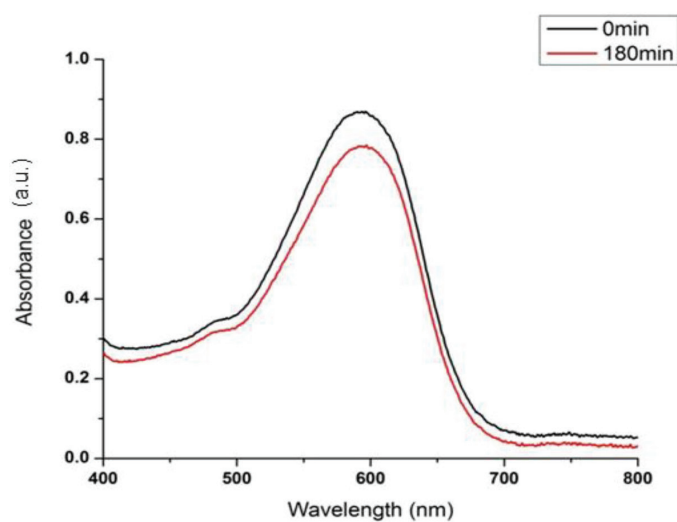
F i g . S 5 – *Time-dependent UV-Vis spectrum of RB5 aqueous solution in presence of silica gel and H$_2$O$_2$ (17.6 mM), instead of catalyst*

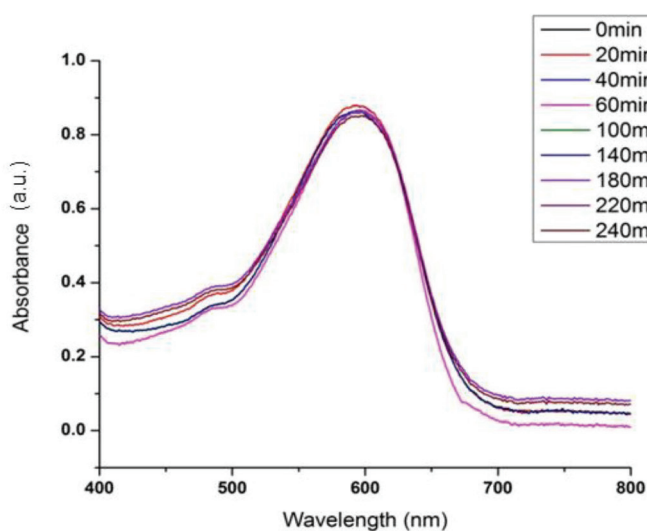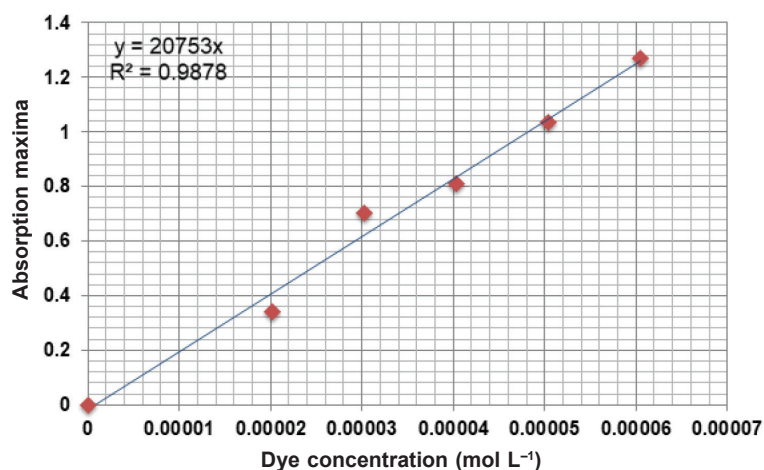Fig. S6 – *Calibration curve- absorbance versus concentration of RB5*
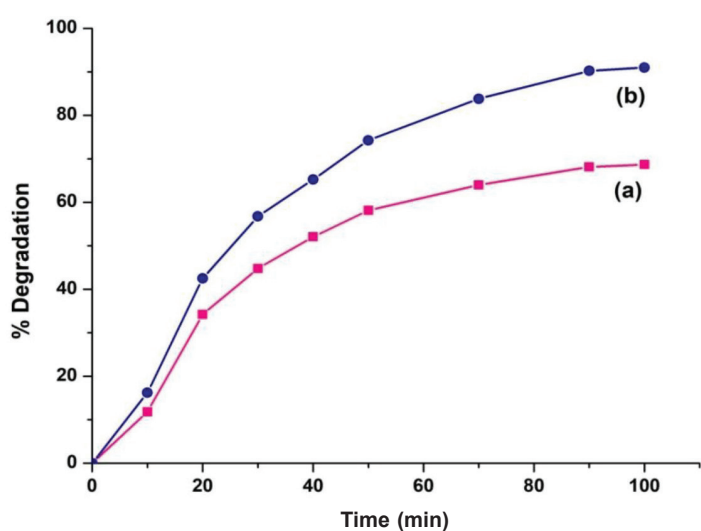
Fig. S7 – *Degradation of RB5 in (a) presence of scavenger, and (b) absence of scavenger (RB5 concentration = 45 ppm, H_2O_2 concentration = 17.6 mM, catalyst concentration = 0.8 g L^{-1}, Scavenger concentration = 0.1 M, T = 35 ± 1 ºC)*
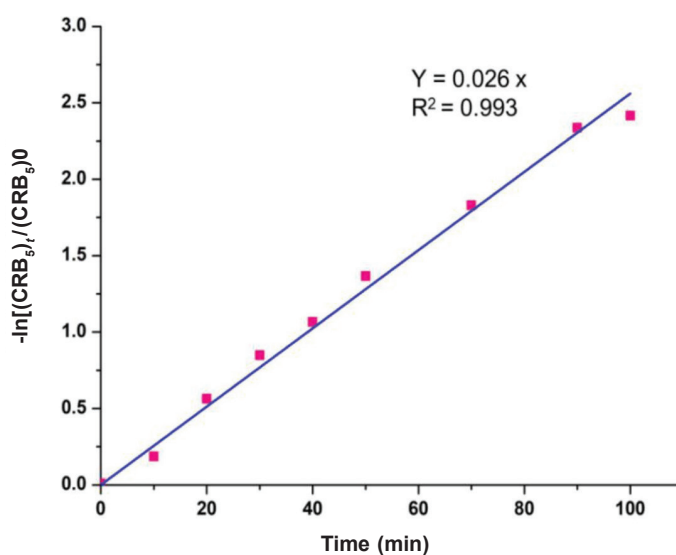
Fig. S8 – *First order plot of $-ln[(C_{RB5})_t/(C_{RB5})_0]$ versus time for degradation of RB5 (RB5 concentration = 45 ppm, H_2O_2 concentration = 17.6 mM, catalyst concentration = 0.8 g L^{-1}, T = 35 ± 1 ºC)*
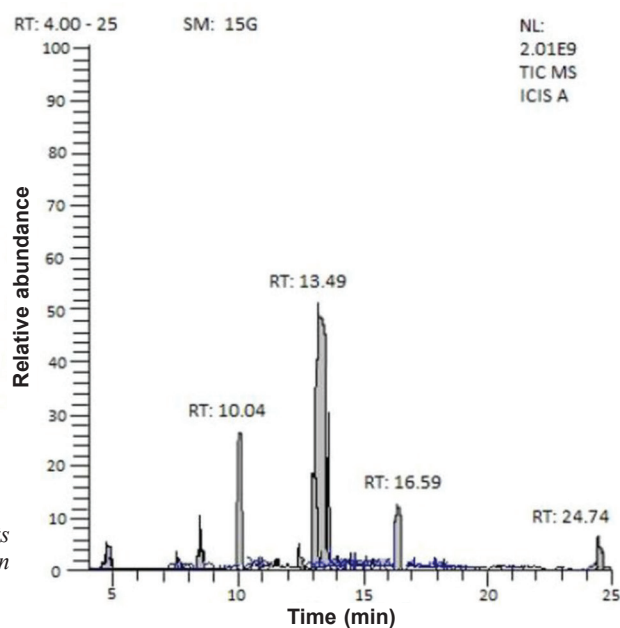
Fig. S9 – *GC graph of products obtained by tetralin conversion*

RT	Compound Name	Area	Area %	Molecular Formula	Molecular Weight	RSI
13.49	1(2H)-Naphthalenone, 3,4-dihydro-	25489251921.81	31.63	$C_{10}H_{10}O$	146	931

RT	Compound Name	Area	Area %	Molecular Formula	Molecular Weight	RSI
13.11	1-Naphthalenol, 1,2,3,4-tetrahydro-	8848308128.40	10.98	$C_{10}H_{12}O$	148	906
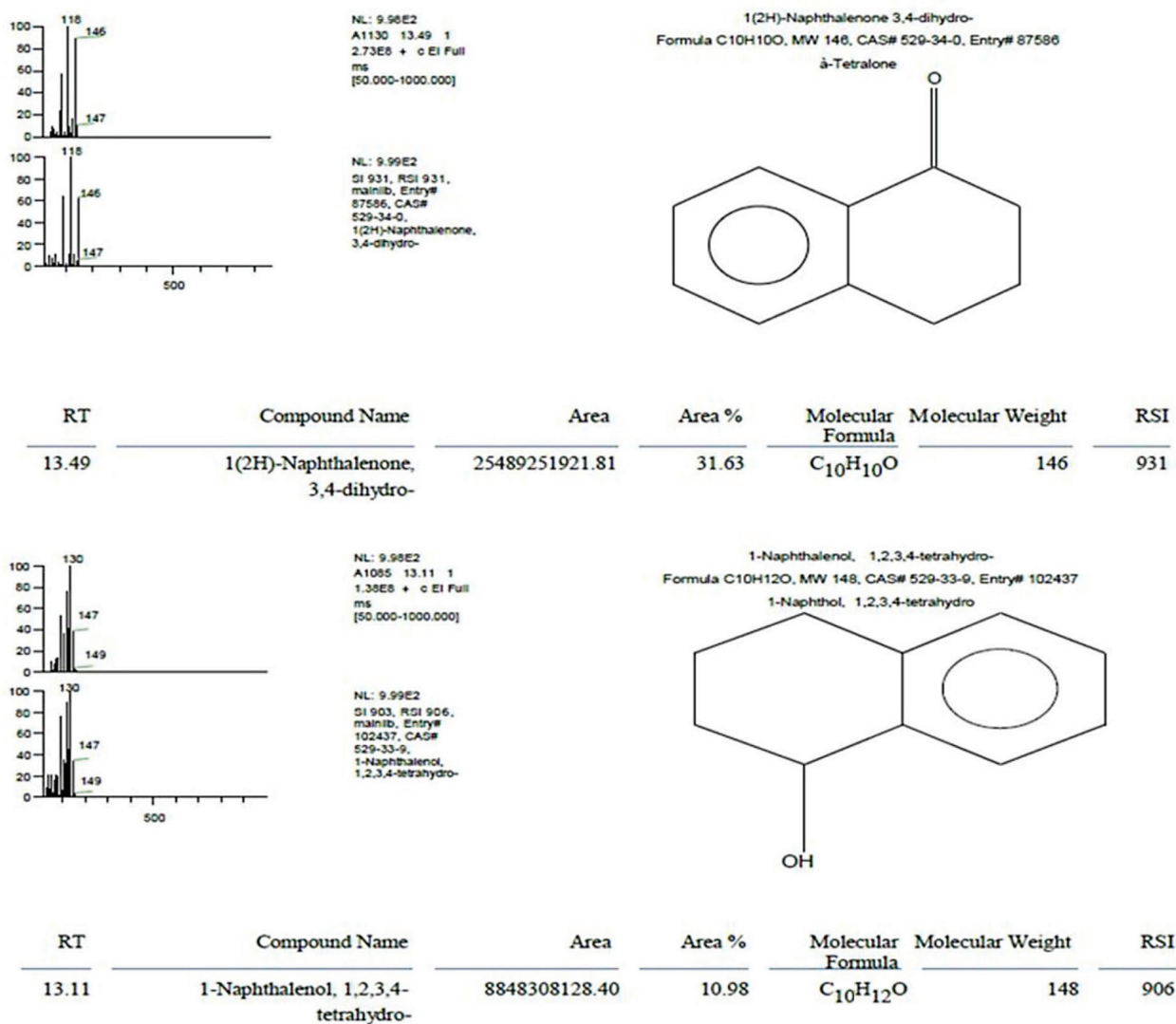
F i g .   S 1 0 – *MS of products obtained by tetralin conversion*
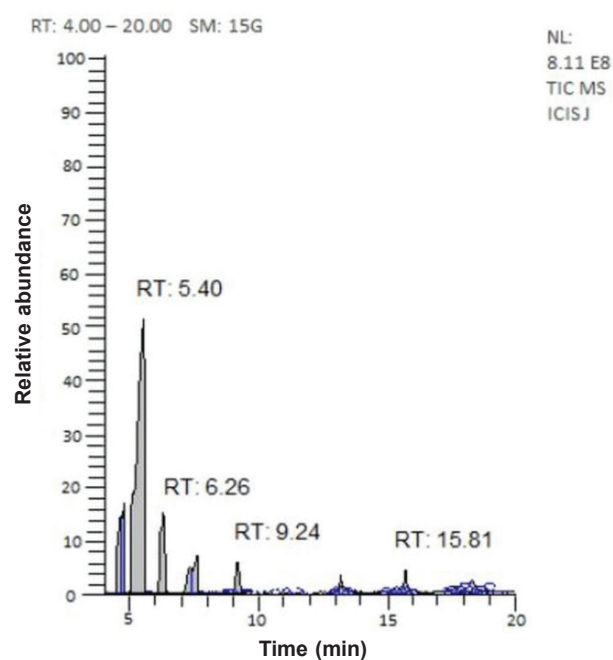
F i g .   S 1 1 – *GC of products obtained by cyclohexane conversion*

Cyclohexanol

Formula $C_6H_{12}O$, MW 100, CAS# 108-93-0, Entry# 23836

Cyclohexyl alcohol ethyl-

RT	Compound Name	Area	Area %	Molecular Formula	Molecular Weight	RSI
4.48	Cyclohexanol	3486530182.15	4.28	$C_6H_{12}O$	100	920

Cyclohexanone

Formula $C_6H_{10}O$, MW 98, CAS# 108-94-1

RT	Compound Name	Area	Area %	Molecular Formula	Molecular Weight	RSI
5.40	Cyclohexanone	25122567948.01	30.84	$C_6H_{10}O$	98	880

Cyclohexanol

Formula $C_6H_{12}O$, MW 100, CAS# 108-93-0, Entry# 23836

Cyclohexyl alcohol ethyl-

RT	Compound Name	Area	Area %	Molecular Formula	Molecular Weight	RSI
6.26	Cyclohexanol	4863220838.18	5.97	$C_6H_{12}O$	100	874

F i g . S 1 2 – *MS of products obtained by cyclohexane conversion*

F i g . S 1 3 *– GC of products obtained by cyclohexanol conversion*

RT	Compound Name	Area	Area %	Molecular Formula	Molecular Weight	RSI
5.40	Cyclohexanone	32669436386.65	40.54	$C_6H_{10}O$	98	880

F i g . S 1 4 *– MS of products obtained by cyclohexanol conversion*

Fig. S15 – *GC of products obtained by cyclopentanol conversion*

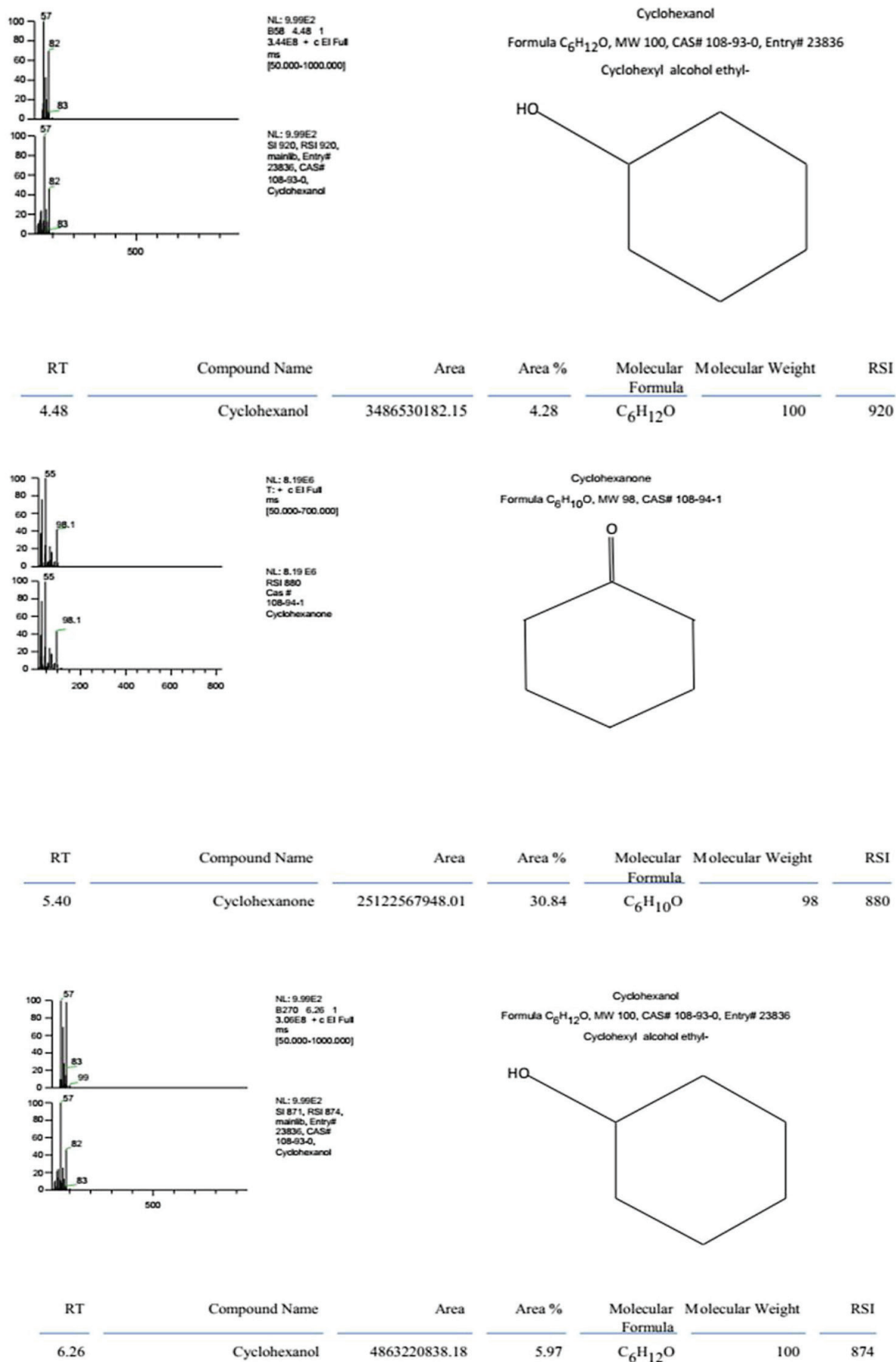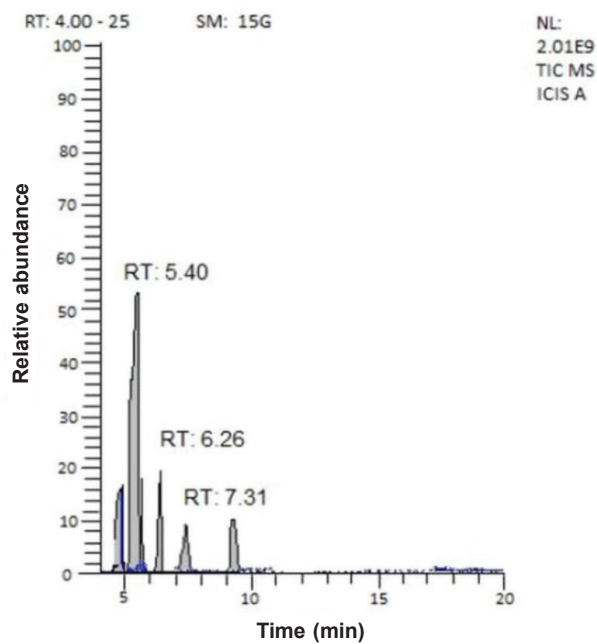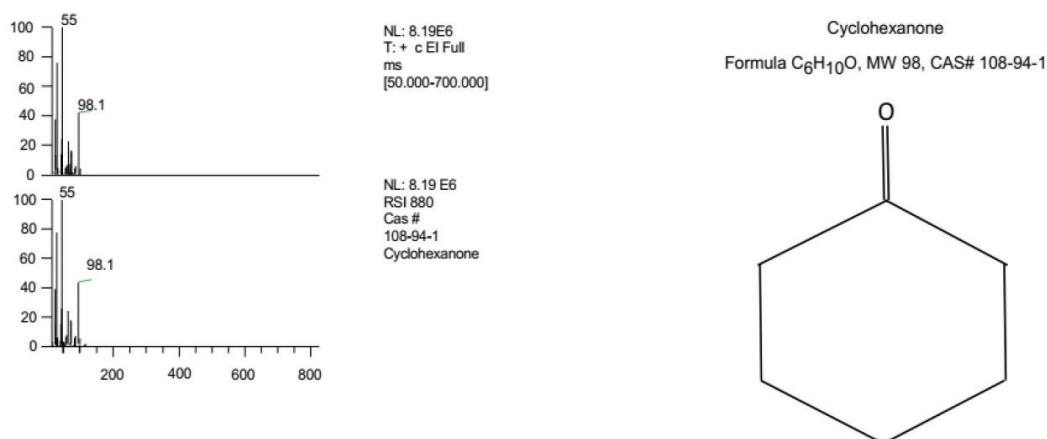| RT	Compound Name	Area	Area %	Molecular Formula	Molecular Weight	RSI
4.29	Cyclopentanone	30977137017.83	38.44	C_5H_8O	84	831
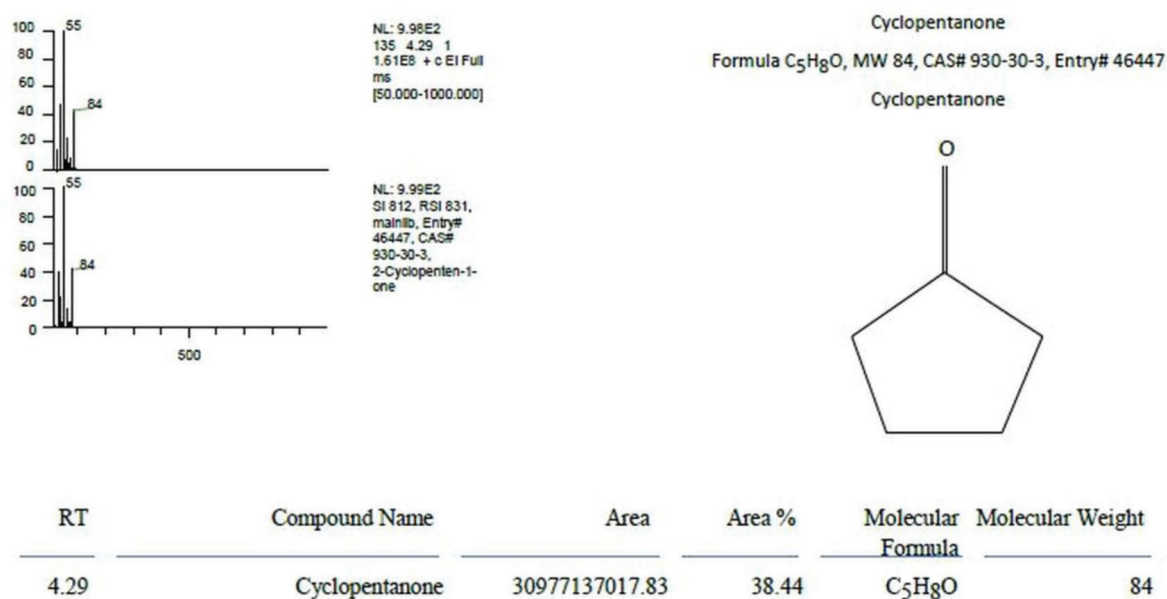
Fig. S16 – *MS of products obtained by cyclopentanol conversion*
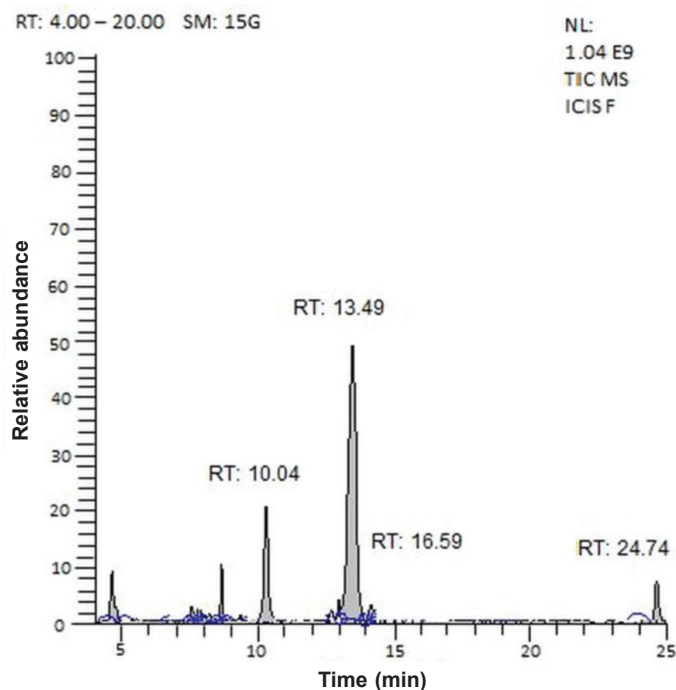
Fig. S17 – *GC of products obtained by tetralin conversion in the 2nd catalytic run*

RT	Compound Name	Area	Area %	Molecular Formula	Molecular Weight	RSI
13.11	1-Naphthalenol, 1,2,3,4-tetrahydro-	8646843917.79	10.73	$C_{10}H_{12}O$	148	906

RT	Compound Name	Area	Area %	Molecular Formula	Molecular Weight	RSI
13.49	1(2H)-Naphthalenone, 3,4-dihydro-	25457017648.01	31.59	$C_{10}H_{10}O$	146	931

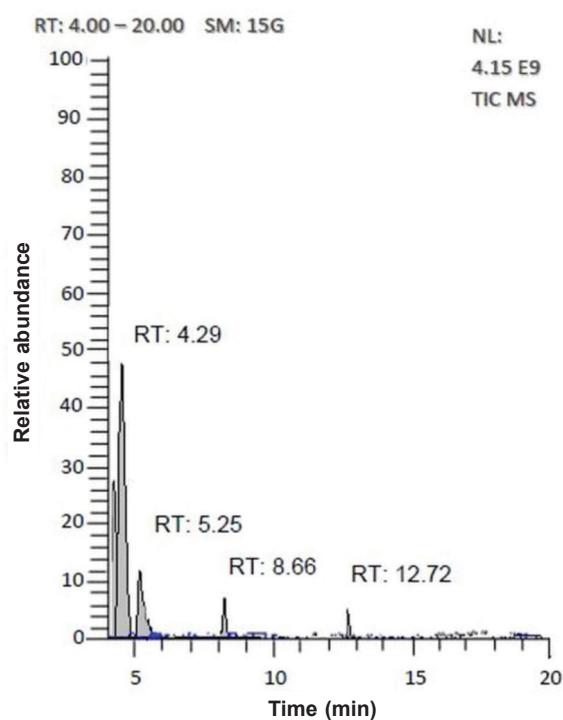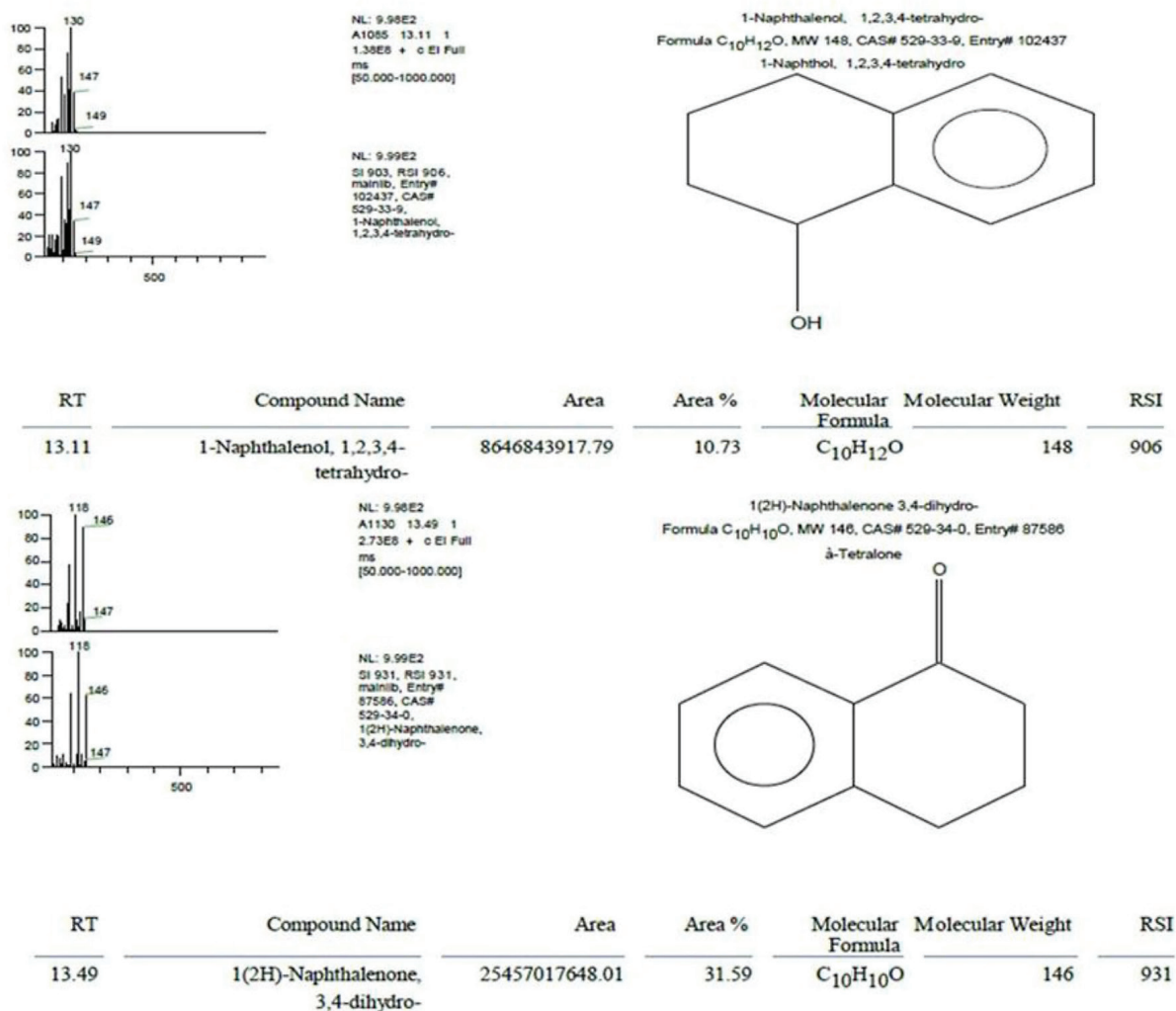Fig. S18 – *MS of products obtained by tetralin conversion in the 2nd catalytic run*
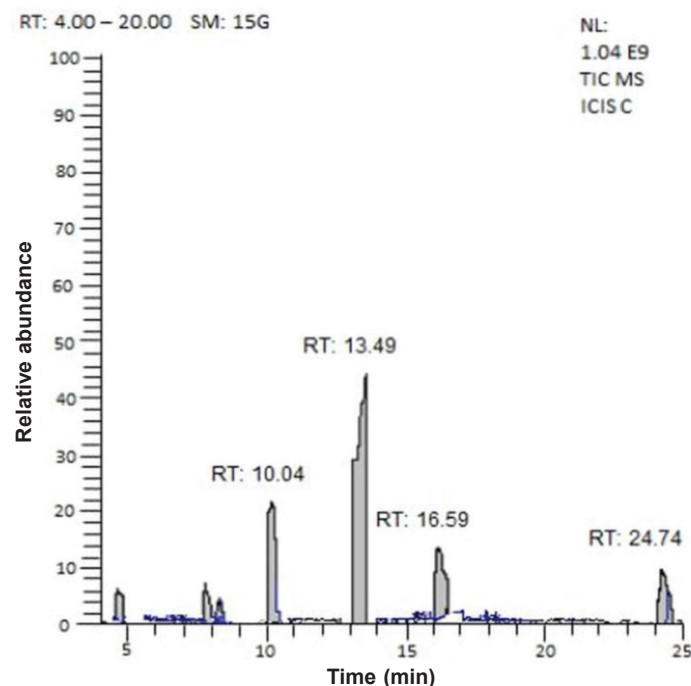
Fig. S19 – *GC of products obtained by tetralin conversion in the 3rd catalytic run*

RT	Compound Name	Area	Area %	Molecular Formula	Molecular Weight	RSI
13.11	1-Naphthalenol, 1,2,3,4-tetrahydro-	8945010949.46	11.10	$C_{10}H_{12}O$	148	906

RT	Compound Name	Area	Area %	Molecular Formula	Molecular Weight	RSI
13.49	1(2H)-Naphthalenone, 3,4-dihydro-	24933210700.56	30.94	$C_{10}H_{10}O$	146	931

Fig. S20 – *MS of products obtained by tetralin conversion in the 3rd catalytic run*

F i g . S 2 1 – *Time-dependent UV-Vis spectrum of RB5 aqueous solution in presence of catalyst (0.8 g L⁻¹), H₂O₂ (17.6 mM), and temperature (35 ± 1 ºC) to observe leaching of metal*

F i g . S 2 2 – *SEM image of reused catalyst after first run*

F i g . S 2 3 – *FTIR of (a) fresh, and (b) reused catalyst after first catalytic run*

References

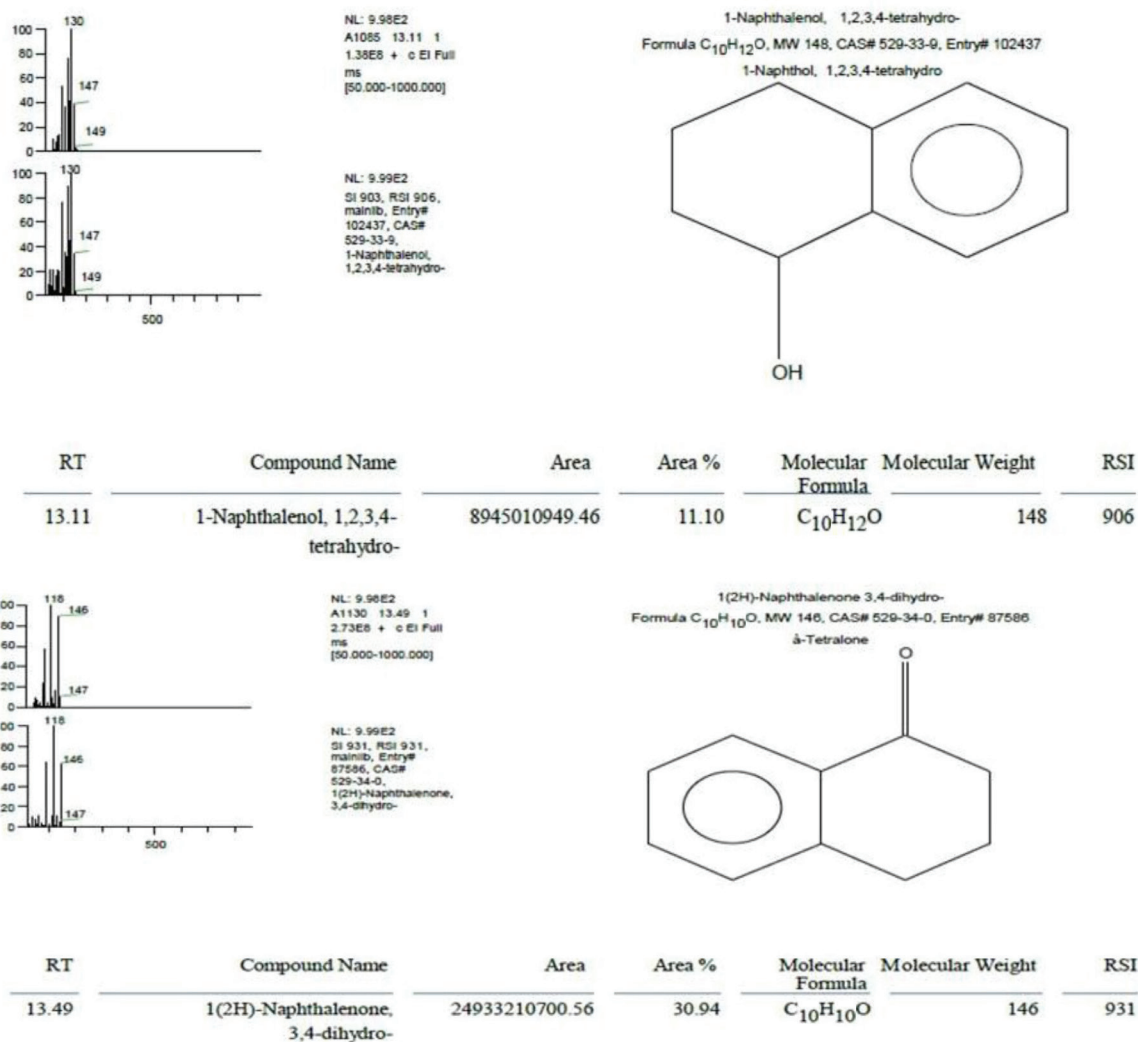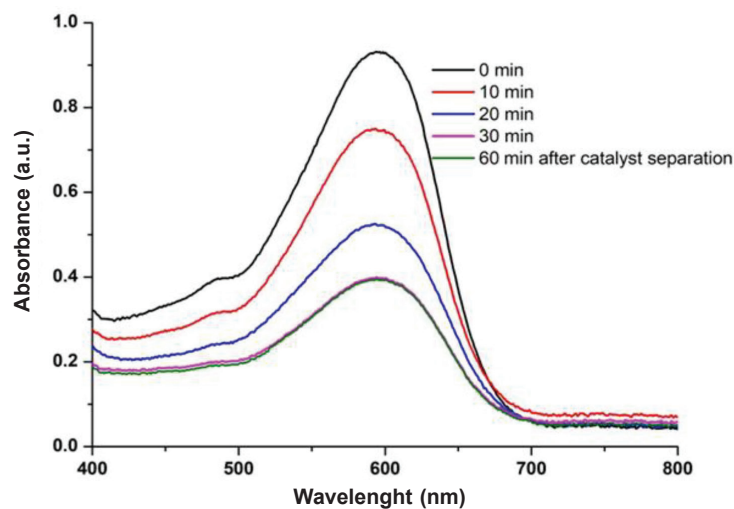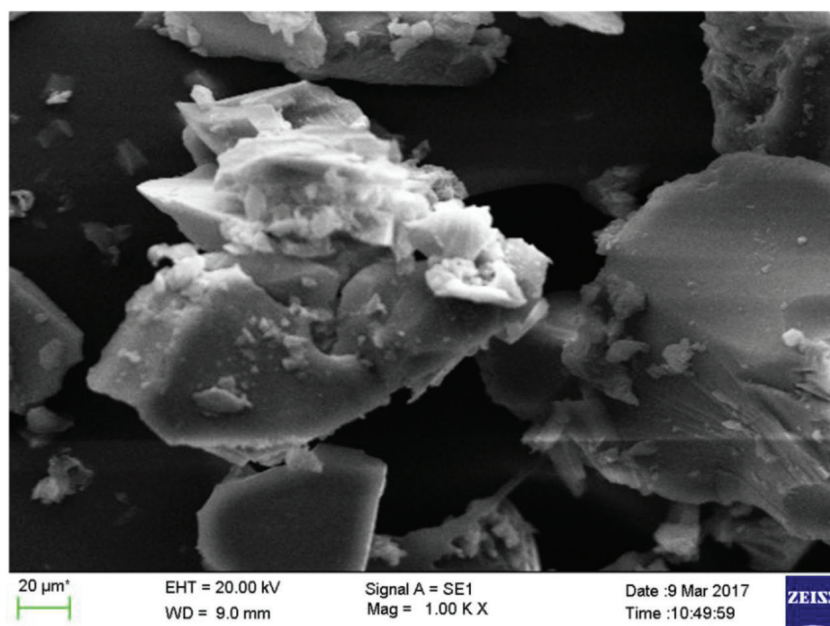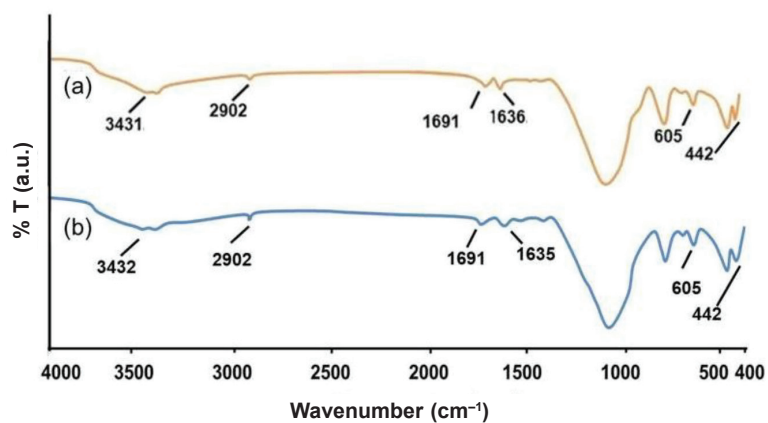1. *Pires de Souza, M. E. P., Ariza, E., Ballester, M., Yoshida, I. V. P., Rocha, L. A., Freire, C. M. A.,* Characterization of organic-inorganic hybrid coatings for corrosion protection of galvanized steel and electroplated ZnFe steel, Materials Research **9** (2006) 59.

2. *Ma, H., Gao, R., Yan, D., Zhao, J., Wei, M.,* Organic–inorganic hybrid fluorescent ultrathin films and their sensor application for nitroaromatic explosives, J. Mater. Chem. C. **1** (2013) 4128.

3. *Noh, J. H., Im, S. H., Heo, J. H., Mandal, T. N., Seok, S.,* Chemical management for colorful, efficient, and stable inorganic–organic hybrid nanostructured solar cells, Nano Lett. **13** (2013) 1764.

4. *Arun, S., Narvi, S. S.,* Immobilization of copper complex by phosphotungstate, their characterization and application in catalysis, J. Pharm. Appl. Chem. **3** (2017) 27.

5. *Junior, J. A. O., Abuçafy, M. P., Manaia, E. B., Lallo da Silva, B., Chiari-Andréo, B. G., Chiavacci, L. A.,* Drug delivery systems obtained from silica based organic-inorganic hybrids, J. Appl. Polym. Sci. **8** (2016) 91.

6. *Urus, S., Purtas, S., Ceyhan, G., Tumer, F.,* Solid phase extraction of Pb(II), Cu(II), Cd(II) and Cr(III) with syringe technique using novel silica-supported bis(diazoimine) ligands, Chem. Eng. J. **220** (2013) 420.

7. *Antony, R., Manickam, S. T. D., Karuppasamy, K., Kollu, P., Chandrasekar, P. V., Balakumar, S.,* Organic–inorganic hybrid catalysts containing new Schiff base for environment friendly cyclohexane oxidation, RSC Adv. **4** (2014) 42816.

8. *Xu, L., Zhou, W., Zhang, L., Li, B., Zang, H., Wang, Y., Li, Y.,* Organic–inorganic hybrid assemblies based on Ti-substituted polyoxometalates for photocatalytic dye degradation, Cryst. Eng. Comm. **17** (2015) 3708.

9. *Dui, X., Yang, W., Wu, X., Kuang, X., Liao, J., Yu, R., Lu, C.,* Two novel POM-based inorganic-organic hybrid compounds: Synthesis, structures, magnetic properties, photodegradation and selective absorption of organic dyes, Dalton Trans. **44** (2015) 9496.

10. *Volikov, A. B., Ponomarenko, S. A., Konstantinov, A. I., Hatfield, K., Perminova, I. V.,* Nature-like solution for removal of direct brown 1 azo dye from aqueous phase using humics-modified silica gel, Chemosphere **145** (2016) 83.

11. *Vinoda, B. M., Vinuth, M., Bodke, Y. D., Manjanna, J.,* Photocatalytic degradation of toxic methyl red dye using silica nanoparticles synthesized from rice husk ash, J. Environ. Anal. Toxicol. **5** (2015) 336.

12. *Abedi, M. H., Ahmadmoazzam, M., Jaafarzadeh, N.,* Removal of cationic tolonium chloride dye using Fe_3O_4 nanoparticles modified with sodium dodecyl sulfate, Chem. Biochem. Eng. Q. **32** (2018) 205.

13. *Puasa, S. W., Ruzitah, M. S., Sharifah, A. S. A. K.,* Competitive removal of Reactive Black 5/Reactive Orange 16 from aqueous solution via micellar-enhanced ultrafiltration, Int. J. Chem. Eng. Appl. **3** (2012) 354.

14. *Zhu, X., Zheng, Y., Chen, Z., Chen, Q., Gao, B., Yu, S.,* Removal of reactive dye from textile effluent through submerged filtration using hollow fiber composite nanofiltration membrane, Desalin. Water. Treat. **51** (2013) 6101.

15. *Morsi, M. S., Al-Sarawy, A. A., Shehab El-Dein, W. A.,* Electrochemical degradation of some organic dyes by electrochemical oxidation on a Pb/PbO_2 electrode, Desalin. Water. Treat. **26** (2011) 301.

16. *Lau, Y. Y., Wong, Y. S., Teng, T. T., Morad, N., Rafatullaha, M., Ong, S. A.,* Degradation of cationic and anionic dyes in coagulation–flocculation process using bi-functionalized silica hybrid with aluminum-ferric as auxiliary agent, RSC Adv. **5** (2015) 34206.

17. *Saharan, V. K., Pandit, A. B., Kumar, P. S. S., Anandan, S.,* Hydrodynamic cavitation as an advanced oxidation technique for the degradation of acid red 88 dye, Ind. Eng. Chem. Res. **51** (2012) 1981.

18. *Jain, A., Lodha, S., Punjabi, P. B., Sharma, V. K., Ameta, S. C.,* A study of catalytic behaviour of aromatic additives on the photo–Fenton degradation of phenol red, J. Chem. Sci. **121** (2009) 1027.

19. *Wang, J. L., Xu, L. J.,* Advanced oxidation processes for wastewater treatment: Formation of hydroxyl radical and application, Crit. Rev. Environ. Sci. Technol. **42** (2012) 251.

20. *Andreozzi, R., Caprio, V., Insola, A., Marotta, R.,* Advanced oxidation processes (AOP) for water purification and recovery, Catal. Today **53** (1999) 51.

21. *Koo, D. H., Kim, M., Chang, S.,* WO_3 nanoparticles on MCM-48 as a highly selective and versatile heterogeneous catalyst for the oxidation of olefins, sulfides, and cyclic ketones, Org. Lett. **7** (2005) 5015.

22. *Arun, S., Narvi, S. S., Pandey, N. D., Pandey, D.,* Solvothermal synthesis of recyclable heterogeneous catalysts by transition metal complex anchored on polyoxometalate keggin unit, Int. J. Sci. Res. Eng. Dev. **1** (2016) 856.

23. *Wang, H., Hu, R., Yang, Y., Gao, M., Wang, Y.,* Direct catalytic synthesis of ε-caprolactam from cyclohexanol using $[n\text{-}C_{16}H_{33}N\ (CH_3)_3]H_2PW_{12}O_{40}$ as a catalyst, Catal. Commun. **70** (2015) 6.

24. *Samir, E. M.,* The uses of cyclopentanone for the synthesis of biologically active pyran, pyridine and thiophene derivatives, OALib Journal **3** (2016) 1.

25. *Covarrubias, Z. A., Cantu, F., Maldonado, L. A.,* A total synthesis of the racemic sesquiterpene parvifoline, J. Org. Chem. **63** (1998) 2918.

26. *Naz, A., Arun, S., Narvi, S. S., Alam, M. S., Singh, A., Bhartiya, P., Dutta, P. K.,* Cu(II)-carboxymethyl chitosan-silane schiff base complex grafted on nano silica: Structural evolution, antibacterial performance and dye degradation ability, Int. J. Biol. Macromol. **110** (2018) 215.

27. *Antony, R., Manickam, S. T. D., Kollu, P., Chandrasekar, P. V., Karuppasamya, K., Balakumara, S.,* Highly dispersed Cu(II), Co(II) and Ni(II) catalysts covalently immobilized on imine-modified silica for cyclohexane oxidation with hydrogen peroxide, RSC Adv. **4** (2014) 24820.

28. *Radi, S., Tighadouini, S., Bacquet, M., Degoutin, S., Cazier, F., Zaghrioui, M., Mabkhot, Y. N.,* Organically modified silica with pyrazole-3-carbaldehyde as a new sorbent for solid-liquid extraction of heavy metals, Molecules **19** (2014) 247.

29. *Arun, T. R., Raman, N.,* Antimicrobial efficacy of phenanthrenequinone based Schiff base complexes incorporating methionine amino acid: Structural elucidation and in vitro bio assay, Spectrochim. Acta A Mol. Biomol. Spectrosc. **127** (2014) 292.

30. *Soylu, M. S., Yesilel, O. Z., Karabulut, B., Büyükgüngör, O.,* Syntheses, spectral, thermal and structural characterization of dinuclear and polynuclear copper(II) orotate complexes, $[Cu_2(HOr)_2(H_2O)_4]$ and $[Cu(l\text{-}HOr)(ba)_2]_n$, Polyhedron **28** (2009) 2487.

31. *Inba, P. J. K., Annaraj, B., Thalamuthu, S., Neelakantan, M. A.,* Cu(II), Ni(II), and Zn(II) Complexes of salan-type ligand containing ester groups: Synthesis, characterization,

electrochemical properties, and *in vitro* biological activities, Bioinorg. Chem. Appl. **2013** (2013) 1.

32. *Radi, S., Tighadouini, S., Bacquet, M., Degoutin, S., Revel, B., Zaghrioui, M.,* Quantitative removal of Zn(II) from aqueous solution and natural water using new silica-immobilized ketoenol–pyridine receptor, J. Environ. Chem. Eng. **3** (2015) 1769.

33. *Singh, G., Rani, S., Arora, A., Sanchita, Duggal, H., Mehta, D.,* Organic-inorganic nano-hybrid decorated by copper (II) incarceration: A versatile catalytic assembly for the swift reduction of aromatic nitro and dye compounds, Mol. Catal. **431** (2017) 15.

34. *Ahmed, A., Lal, R. A.,* Synthesis, characterization and electrochemical studies of copper(II) complexes derived from succinoyl- and adipoyldihydrazones, Arabian J. Chem. **10** (2017) S901.

35. *Kivelson D., Neiman R.,* ESR studies on the bonding in copper complexes, J. Chem. Phys. **35** (1961) 149.

36. *Verma, P., Shah, V., Baldrian, P., Gabriel, J., Stopka, P., Trnka, T., Nerud, F.,* Decolorization of synthetic dyes using a copper complex with glucaric acid, Chemosphere **54** (2004) 291.

37. *Shah, V., Verma, P., Stopka, P., Gabriel, J., Baldrian, P., Nerud, F.,* Decolorization of dyes with copper(II)/organic acid/hydrogen peroxide systems, Appl Catal B: Environmental **46** (2003) 287.

38. *Perez-Benito, J. F.,* Reaction pathways in the decomposition of hydrogen peroxide catalyzed by copper(II), J. Inorg. Biochem. **98** (2004) 430.

39. *Baldrian, P., Merhautova, V., Gabriel, J., Nerud, F., Stopka, P., Hruby, M., Benes, M. J.,* Decolorization of synthetic dyes by hydrogen peroxide with heterogeneous catalysis by mixed iron oxides, Applied Catalysis B: Environmental **66** (2006) 258.

40. *Lin, T. Y., Wu, C. H.,* Activation of hydrogen peroxide in copper(II)/amino acid/H$_2$O$_2$ systems: Effects of pH and copper speciation, J. Catal. **232** (2005) 117.

41. *Lucas, M. S., Peres, J. A.,* Decolorization of the azo dye Reactive Black 5 by Fenton and photo-Fenton oxidation, Dyes Pigm. **71** (2006) 236.

42. *Nasuha, N., Ismail, S., Hameed, B. H.,* Activated electric arc furnace slag as an efficient and reusable heterogeneous Fenton-like catalyst for the degradation of Reactive Black 5, J. Taiwan Inst. Chem. Eng. **67** (2016) 235.

43. *Ramirez, J. H., Maldonado-Hódar, F. J., Pérez-Cadenas, A. F., Moreno-Castilla, C., Costa, C. A., Madeira, L. M.,* Azo-dye Orange II degradation by heterogeneous Fenton-like reaction using carbon-Fe catalysts, Applied Catalysis B: Environmental **75** (2007) 312.

44. *Soon, A. N., Hameed, B. H.,* Degradation of Acid Blue 29 in visible light radiation using iron modified mesoporous silica as heterogeneous Photo-Fenton catalyst, Applied Catalysis A: General **450** (2013) 96.

45. *Wang, Y., Wang, J., Zou, H., Xie, Y.,* Heterogeneous activation of hydrogen peroxide using γ -Al$_2$O$_3$ supported bimetallic Fe, Mn for the degradation of reactive black 5, RSC Adv. **6** (2016) 15394.

46. *Modi, C. K., Trivedi, P. M.,* Zeolite-Y entrapped Ru(III) and Fe(III) complexes as heterogeneous catalysts for catalytic oxidation of cyclohexane reaction, Arabian J. Chem. **10** (2017) S1452.

47. *Arun, S., Singh, V. K., Naz, A., Narvi, S. S., Dutta, P. K.,* A comparative catalytic study using different metal ions by incorporating functionalized metallosalen into the lacunary position of Keggin polyoxometalate, J. Indian Chem. Soc. **98** (2021) 100118.

48. *Lau, Y. -Y., Wong, Y. -S., Ang, T. -Z., Ong, S. -A., Lutpi, N. A., Ho, L. -N.,* Degradation reaction of Diazo reactive black 5 dye with copper (II) sulfate catalyst in thermolysis treatment, Environ. Sci. Pollut. Res. **25** (2018) 7067.

49. *Salem, I. A., Shaltout, M. H., Zaki, A. B.,* Homogeneous and heterogeneous catalytic oxidation of some azo dyes using copper(II) ions, Spectrochim. Acta, Part A. **227** (2020) 117618.